



Two-dimensional nanocomposite materials for photoelectrochemical water-splitting applications: An overview



Tse-Wei Chen^a, Shen-Ming Chen^{b,*}, Palraj Kalimuthu^{c,*}, Ganesan Anushya^d, Ramanujam Kannan^e, Abdullah G. Al-Sehemi^f, Vinitha Mariyappan^g, Saranvignesh Alargarsamy^b, Mohammed Mujahid Alam^f, Suganya Jeyabal^h, Thavasimuthu Chinnakan Maheshⁱ, Rasu Ramachandran^j

^a Department of Materials, Imperial College London, London SW7 2AZ, UK

^b Department of Chemical Engineering and Biotechnology, National Taipei University of Technology, Taipei 10608, Taiwan

^c Vital Trace Medical Technology Manufacture, 2 Action Road, Malaga, Perth, WA 6090, Australia

^d Department of Physics, St. Joseph College of Engineering, Sripurumbudur, Chennai 602 117, India

^e Department of Chemistry, Sri Kumaragurupara Swamigal Arts College, Srivaikuntam, Thoothukudi 628619, India

^f Department of Chemistry, College of Science, King Khalid University, Abha 61413, Saudi Arabia

^g Advanced Institute of Manufacturing with High-tech Innovations and Department of Mechanical Engineering, National Chung Cheng University, Chiayi 621301, Taiwan, ROC

^h Department of Chemistry, School of Arts and Science, Vinayaga Mission, Chennai Campus, VMRFDU, 603104, India

ⁱ Department of Zoology, Vivekananda College, Agasteeswaram, Kanyakumari, India

^j Department of Chemistry, The Madura College (Affiliated to Madurai Kamaraj University), Vidya Nagar, Madurai 625011, India

ARTICLE INFO

Keywords:

2D nanomaterials
Fabrication techniques
Water-splitting
Current density
Tafel slope
Cyclic stability
Photoelectrochemical
Electrochemical

ABSTRACT

Recently, researchers have directed considerable attention towards developing eco-friendly fuel energy technology suitable for widespread implementation. Photoelectrochemical (PEC) based water-splitting technology has been found to play a crucial role in converting solar energy into chemical energy. Therefore, water-splitting through the PEC process is considered one of the most effective methods for generating eco-friendly and sustainable energy sources. Among the various nanomaterials-based photo-electrocatalysts reported in the literature, two-dimensional (2D) materials-based photoelectrocatalysts have been extensively applied across numerous domains, serving as cost-effective and efficient catalysts. Their adaptable structures and compositions provide significant prospects and avenues to create tailored electrocatalysts, presenting abundant opportunities for design strategies. Extensive discussions have been covered in this review regarding various methods employed for synthesizing 2D materials-based photoelectrocatalysts and their hybrid materials. These discussions also encompass diverse strategies to alter the physicochemical properties of the developed photoelectrocatalysts. In addition, this review ultimately offers valuable insights into the potential applications of various 2D-based composites and their merits and limitations. The review also outlines some proposed research directions that will be pursued in this field in the future.

1. Introduction

Globally, fossil fuels are currently a pressing issue as they contribute to greenhouse gas emissions and environmental pollution [1,2]. In light of this, there is an urgent need for an alternative energy source to meet the world's energy needs. Human survival and advancement are predominantly tied to energy derived from fuel. However, the resultant

environmental degradation caused by prolonged dependence on traditional energy sources has become widespread. Clean and green hydrogen energy emerges as the most favorable alternative to fossil fuels due to its high-energy density and absence of secondary pollution. It stands out as the most promising substitute, offering a clean solution for energy needs [3,4]. Generally, hydrogen fuels are produced using a variety of methods, such as coal gasification [5], natural gas reforming

* Corresponding authors.

E-mail addresses: smchen@ntut.edu.tw (S.-M. Chen), kalimuthu.palraj@vitaltrace.com.au (P. Kalimuthu), [\(R. Ramachandran\).](mailto:ramachandran@maduracollege.edu.in)

[6], electrocatalysis [7], and PEC processes [8], among others.

Solar energy conversion to produce green fuel hydrogen has arisen as an efficient remedy to address global energy needs and environmental pollution. We recently reviewed a range of nanomaterials and composites used for water-splitting applications [9–12]. Among the various technologies enabling solar-to-hydrogen conversion, PEC water splitting emerges as the most viable approach for generating environmentally friendly, clean, and sustainable fuel energy [13–15]. Compared to traditional methods, the PEC water splitting technique has demonstrated superiority due to its convenience, minimal bias voltage requirement, low energy consumption, and high efficiency [16]. In recent times, few novel electrode materials categorized as zero-dimensional [17], one-dimensional [18], and two-dimensional (2D) [19] have been devoted to advancing the PEC water-splitting reaction. Among these, the strategic integration of 2D electrocatalysts has emerged as one of the most promising approaches to enhance the PEC water-splitting process for the production of environmentally friendly energy fuels.

For instance, Rao *et al.* reported the fabrication of wide band gap semiconductor-based graphitic carbon nitride ($\text{g-C}_3\text{N}_4$) materials through the thermal pyrolysis method [20]. The resulting $\text{g-C}_3\text{N}_4$ photoelectrode demonstrated an ability to improve the separation and transfer of photo-generated charge carriers, facilitating the production of hydrogen fuels via the PEC water-splitting process. Furthermore, the different kinds of 2D based electrodes such as graphitic carbon nitride [21,22], layered double hydroxides [23,24], nanosheets [25], graphene oxide [26,27], metal chalcogenides [28,29], MXene [30,31], etc., have been fabricated using diverse techniques. These materials are regarded as highly efficient photoelectrocatalysts, significantly advancing solar energy conversion through photoelectrochemical water-splitting reactions. Further, Yin and coworkers utilized a facile hydrothermal method to create a Janus-structured cobalt-nanoparticle-coupled Ti_3C_2 MXene quantum dot (Co-MQD) [32]. The Schottky catalyst Co-MQD-48 demonstrates significantly enhanced photocurrent density and carrier migration efficiency, measuring 2.99 mA cm^{-2} and 87.56%, respectively. In another report, Ashraf and coworkers developed a composite material involving polymeric carbon nitrides (PCN) integrated with highly reduced graphene oxide (HGO) [33]. Remarkably, the PCN/HRG nanocomposite exhibited a superior photocurrent density of $71 \mu\text{A cm}^{-2}$ compared to melon's $24 \mu\text{A cm}^{-2}$ under alkaline conditions. Shen and colleagues recently used a cost-effective electrodeposition method to fabricate a Mo-doped NiFe-layered double hydroxide (LDH) on a

NiOx/Ni-protected Si photoanode [34]. The incorporation of Mo during the fabrication process notably increased the presence of oxygen vacancies. Furthermore, Mo leaching induced a dynamic self-reconstruction of the surface under conditions relevant to PEC oxygen evolution reactions (OER). This alteration enhanced PEC performance, evidenced by an onset potential of 0.87 V vs. the reversible hydrogen electrode (RHE), a substantial photocurrent density reaching 39.3 mA cm^{-2} at 1.23 V vs. RHE. The various fabrication techniques of electro(photo)catalysts and their operational conditions, activity and stability are summarized in Table 1.

This review provides a comprehensive overview of the fabrication, properties, design, and synthesis of 2D electrode materials. It also outlines the potential trends for various types of 2D-based heterogeneous (graphitic carbon nitride, transition metal oxides, perovskites, molybdenum carbide, layered double hydroxides, nanosheets, graphene oxide, transition metal chalcogenides, and MXene) photocatalytic materials in the exploration of PEC water-splitting reactions. Initially, our focus was on exploring the promising characteristics exhibited by various types of 2D-based electrode materials. Subsequently, we emphasized different approaches for modifying these materials to enhance the photoelectrocatalytic activity of 2D-based photocatalytic materials. Finally, this review addresses the major challenges associated with 2D-based photocatalysts while exploring future research opportunities.

2. Two-dimensional nanocomposite electrode materials

So far, various 2D nanocomposite materials have been explored for their potential in (photo)electrochemical water-splitting applications. This section delves into the analysis of fabrication techniques, catalytic mechanisms and efficiency, stability, and scalability of different 2D nanocomposite electrode materials. These materials include graphene, graphitic carbon nitride, transition metal oxides, metal nanosheets, hexagonal boron nitride, perovskite, MXene, layered double hydroxides, and metal chalcogenides.

2.1. Graphene-based composite materials

Graphene is a singular layer of sp^2 hybridized carbon atoms forming a two-dimensional (2D) sheet with remarkable characteristics. Its extensive specific surface area of $2630 \text{ m}^2 \text{ g}^{-1}$, along with exceptional carrier mobility at around $15,000 \text{ cm}^2 \text{ V}^{-1} \text{ s}^{-1}$ at room temperature, stands out. Furthermore, it exhibits commendable optical transparency

Table 1

Comparision of various (photo) electrocatalysts for their electrolytic conditions and water-splitting activities.

Electrocatalysts	Fabrication techniques	Electrolytes (M)	Onset potential (V)	Tafel slope (mV dec ⁻¹)	Current density (mA cm ⁻²)	Stability	Ref.
^a $\text{Ni}_{2/3}\text{Fe}_{1/3}$ -rGO	Precipitation	1 M KOH	0.23	42	10	36000 s	[51]
^b CoP/Graphene	In situ	1 M KOH	0.125	118	10	24 hrs	[52]
^c $\text{Co}_{0.4}\text{Fe}_{0.6}$ LDH/g-CN _x	One-pot co-precipitation	1 M KOH	0.28	29	10	-	[63]
^d $\text{FeO}_x/\text{NF-Li}$	Hydrothermal	1 M NaOH	0.239	102	100	12 hrs	[75]
^e ECT- $\text{Co}_{0.37}\text{Ni}_{0.26}\text{Fe}_{0.37}$ O	Electrochemical	1 M KOH	0.232	37.6	10	100 hrs	[76]
^f NiSe_2/CC	Hydrothermal	1 M KOH	1.531	33.2	10	1000 clys	[84]
^g FeCH@GDY/NF	Hydrothermal	1 M KOH	0.260	54.5	100	10,000 clys	[85]
^h Co-P@NC-800	Template	1 M KOH	0.370	79	10	3 hrs	[86]
ⁱ $\text{Ni}_{2/3}\text{Fe}_{1/3}$ -rGO LDH	Precipitation/Hummers	1 M KOH	0.21	40	10	10,000 s	[87]
^j NiFe (oxy)hydroxide	Roll-to-roll	1 M NaOH	0.250	22.2	10	500 s	[107]

^a $\text{Ni}_{2/3}\text{Fe}_{1/3}$ -rGO-Nickel-iron based reduced graphene oxide;

^b CoP/Graphene-Cobalt phosphide-based graphene composite;

^c $\text{Co}_{0.4}\text{Fe}_{0.6}$ LDH/g-CN_x-Cobalt iron layered double hydroxide based graphitic carbon nitride composite;

^d $\text{FeO}_x/\text{NF-Li}$ -Transition metal oxide based nickel foam with lithium ion;

^e ECT- $\text{Co}_{0.37}\text{Ni}_{0.26}\text{Fe}_{0.37}$ O- Electrochemically oxidized transition metal oxide;

^f NiSe_2/CC -Nickel selenide based carbon cloth;

^g FeCH@GDY/NF -Ultrathin graphdyne based iron carbonate hydroxide nanosheet nickel foam;

^h Co-P@NC-800-Cobalt phosphide based mesoporous nitrogen doped mesoporous graphitic carbon;

ⁱ $\text{Ni}_{2/3}\text{Fe}_{1/3}$ -rGO LDH-Bimetallic layered double hydroxide based reduced graphene oxide composite;

^j NiFe (oxy)hydroxide-Bimetallic (oxy)hydroxide electrode.

of 97.7%, impressive Young's modulus of 1 Tpa, and notable thermal conductivity. Graphene-derived substances show great potential in electrochemical uses because of their fascinating attributes. These include an easily adjustable surface area, exceptional electrical conductivity, robust chemical stability, and superb mechanical performance [35–38]. Consequently, substantial activities have been dedicated to developing varied fabrication techniques (Hummer's [39], sol-gel [40], electrochemical [41] and hydrothermal [42]) for graphene and its incorporation with other functional materials. This recreation aims to broaden the scope of graphene applications. The utilization of graphene-based electrode materials extent diverse electrochemical applications such as electrochemical sensors [43], supercapacitors [44], lithium-ion batteries [45], and dye-sensitized solar cells [46], among others. The rapid and convenient laser-induced technique is employed to fabricate a composite of nitrogen-doped porous graphene supported by cobalt nanoparticles within a metal-organic framework under typical room temperature conditions in an atmospheric air setting. The prompt preparative approach coupled with impressive performances suggests the promising potential of this method in facile and rapid electrode fabrication, specifically for electrocatalysis [47].

Likewise, there's a drive for creating affordable and high-performing cobalt-chromium nanoparticles embedded with graphene nanotubes using an economically viable method. The graphene tube has a diameter of 100 nm. Electrochemical behavior relies significantly on chromium due to its ability to resist corrosion, enhance catalytic sites, and ensure extended stability and remarkable activity in the long run [48]. Using a scalable hydrothermal technique, a composite of graphene quantum dots supported by cobalt nanoparticles is synthesized. This economically feasible method presents a new path to produce electrocatalysts based on quantum dots, offering possibilities to investigate fresh synthesis approaches for these substances. Moreover, it opens avenues for exploring untapped materials for clean energy and environmental applications [49]. The chemical vapor deposition (CVD) strategy was used to produce a stacked nanofilm G-BNG, composed of pure graphene (G) layered atop boron and nitrogen (BN)-codoped graphene (BNG). This innovative G-BNG structure has emerged as a highly promising option for creating durable and consistent electrocatalysts specifically for Oxygen Evolution Reaction (OER). In this study, they explore a deeper understanding of the fundamental mechanism behind the OER efficiency exhibited by this layered catalyst. The investigation involved a meticulous correlation between the structural and chemical characteristics of the catalyst layer and its performance in facilitating the OER process [50].

A cost-effective homogeneous precipitation method was employed for the fabrication of 3D transition metal layered double hydroxides (LDHs) [51]. A step-by-step protocol is illustrated in Fig. 1 for the construction of alternatively stacked graphene and NiFe LDH nanosheets. These LDHs comprised varying proportions of Ni and Fe and were successfully produced on an economical scale. The resulting exfoliated nanosheets of Ni-Fe LDHs were then combined in a hetero assembly with both graphene oxide (GO) and reduced graphene oxide (rGO), forming superlattice-like hybrids. These hybrids featured a unique arrangement

where oppositely charged nanosheets were stacked in an alternating face-to-face sequence. The Ni₂/3Fe1/3-rGO superlattice composites demonstrated exceptional performance upon conducting electrocatalytic activity assessments for OER. Specifically, these composites exhibited a remarkably low overpotential of 0.21 V and a Tafel slope measuring 40 mV/decade. The integration of GO/rGO serves two significant purposes in enhancing the performance of LDH nanosheets in electrochemical applications. Firstly, it impedes the aggregation of LDH nanosheets, thereby effectively isolating them and augmenting the electrochemical active surface areas. Secondly, the direct and interfacial contact between LDH nanosheets and GO/rGO at a molecular scale within the superlattices generates a synergistic effect, particularly facilitating the OER process. This synergistic effect is notably pronounced as LDH nanosheets are able to integrate more intimately with rGO as a result of the removal of oxygen-containing functional groups from GO.

The CoP/graphene composite was synthesized using a co-precipitation and in-situ phosphorization method with α -Co(OH)₂ and GO as starting materials (depicted in Fig. 2a) [52]. HR-TEM imaging revealed a 2D layered structure ensuring uniform attachment of α -Co(OH)₂ nanosheets onto the GO surface, forming a sandwich-like arrangement (Fig. 2b). This configuration led to the creation of fine nanoparticles, crucial for exposing more active sites vital for CoP's role as an electrocatalyst in water splitting. Consequently, the CoP/graphene composite demonstrated outstanding electrocatalytic performance in 1 M KOH, excelling in the HER and OER processes. Notably, the composite exhibited overpotentials of 119 mV for HER and 374 mV for OER in 1 M KOH (Fig. 2c). Moreover, the composite stability tests displayed the remarkable stability of CoP/graphene//CoP/graphene in 1 M KOH under a constant voltage of 1.8 V (Fig. 2d). The catalyst maintained the overall water-splitting process for 24 hours without significant degradation in current density, validating its robust endurance.

2.2. Graphitic carbon nitride (g -C₃N₄) based composite materials

The integration of semiconductor-based electrode materials with various types of nanomaterials represents a promising avenue for advancing energy storage technology and mitigating environmental pollution. Cost-effective, flexible, and stable photocatalytic electrode materials offer significant advantages in green energy technology due to their unique structural arrangements and exceptional photoelectrocatalytic activity [53–55]. In general, Graphitic carbon nitride (g -C₃N₄) based materials exhibit numerous advantages over conventional electrode materials. These include a unique electronic structure, superior optical properties, good adaptability, outstanding mechanical properties, excellent porous and electronic properties, and long cyclic durability [56]. Recent advancements have demonstrated that a layered structure within a photocatalytic system can efficiently generate fuel energy from sunlight, offering a promising to store solar energy. Further, g -C₃N₄-based electrodes are considered highly promising for their potential in energy conversion, particularly in the production of hydrogen fuels through large-scale photocatalytic water-splitting processes [57,

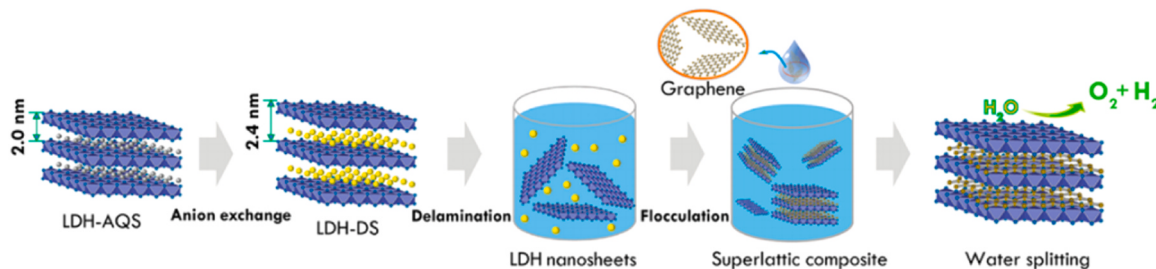


Fig. 1. Fabrication protocol of alternatively stacked graphene and NiFe LDH nanosheets. Reprinted with permission from [51]. Copyright (2015), American Chemical Society.

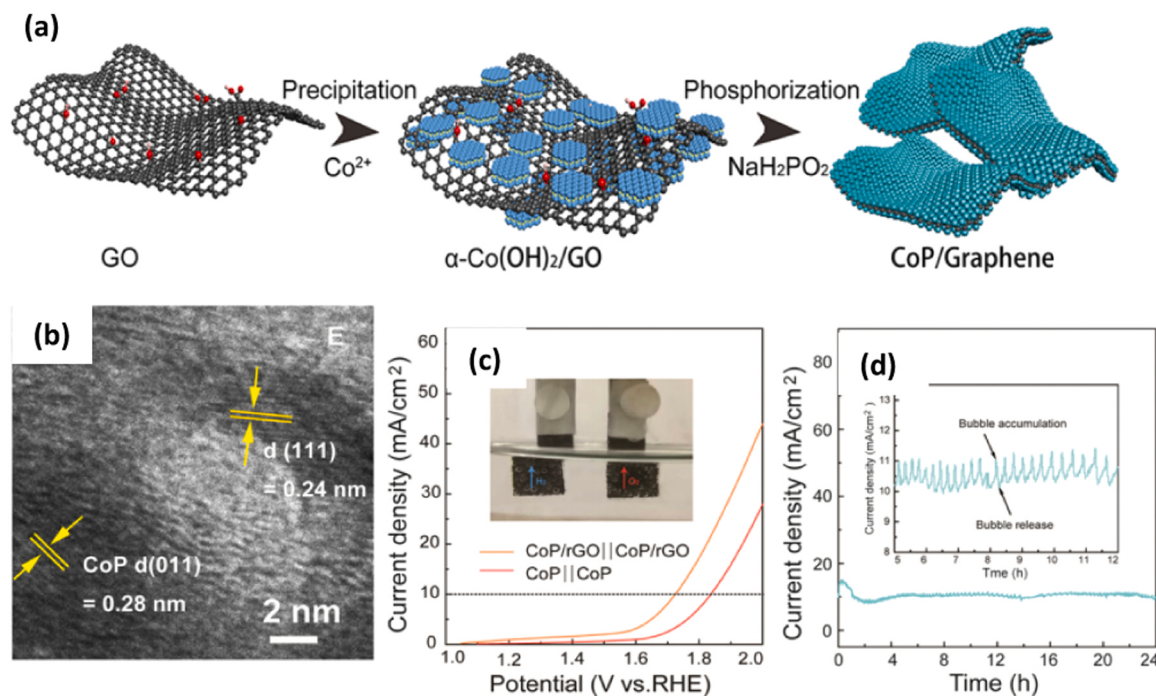


Fig. 2. (a) Fabrication protocol of sandwiched CoP/Graphene heterostructure, (b) HR-TEM image of CoP/graphene, (c) Polarization curves of CoP/graphene||CoP/graphene and CoP||CoP for water splitting in 1.0 M KOH (d) Chronoamperometric curve of CoP/graphene||CoP/graphene at an applied potential of 1.8 V. Reprinted with permission from [52]. Copyright (2020), American Chemical Society.

[58]. Li *et al.* fabricated a heterostructured electrocatalyst by anchoring cobalt onto molybdenum nitride-based graphitic carbon nitride ($\text{Mo}_2\text{N}/\text{Co-C}_3\text{N}_4$) through a heat treatment process [59]. Consequently, the $\text{Mo}_2\text{N}/\text{Co-C}_3\text{N}_4$ catalyst exhibited remarkable bifunctional activity, enhancing the overall efficiency of the water-splitting process.

A novel approach was employed to fabricate a high surface area layered g-C₃N₄ material enhanced by the incorporation of inverse spinel-type Co_2SnO_4 through a straightforward one-pot hydrothermal route [60]. The resulting $\text{Co}_2\text{SnO}_4/\text{g-C}_3\text{N}_4$ nanohybrid electrode exhibited outstanding performance in both HER and OER, achieving low overpotentials of 41 mV for HER and 260 mV for OER. Furthermore, Wu *et al.* reported the synthesis of efficient bifunctional cobalt nitride supported graphitic carbon composites using self-template strategies [61].

The developed composite demonstrated the ability to achieve a current density of 10 mA cm^{-2} with a low overpotential of 149 mV for the HER and 248 mV for the OER, respectively. In another report, a bifunctional electrocatalyst, nickel and molybdenum carbide supported nitrogen-doped graphitized carbon (Ni-Mo₂C/NC) was developed using a one-step pyrolysis technique with fish scales derivative as a carbon source [62]. The developed electrocatalyst exhibited excellent electrochemical performance for both OER and HER. The synergistic effect between Ni, Mo₂C, and NC has been shown to increase the active sites, thereby reducing the energy barrier for electrochemical reactions and facilitating electron transfer. The catalytic achieved an overpotential of 310 mV and 101 mV (at a current density of 10 mA cm^{-2}) for OER and HER, respectively, in alkaline electrolytes. In addition, Ni-Mo₂C/NC can

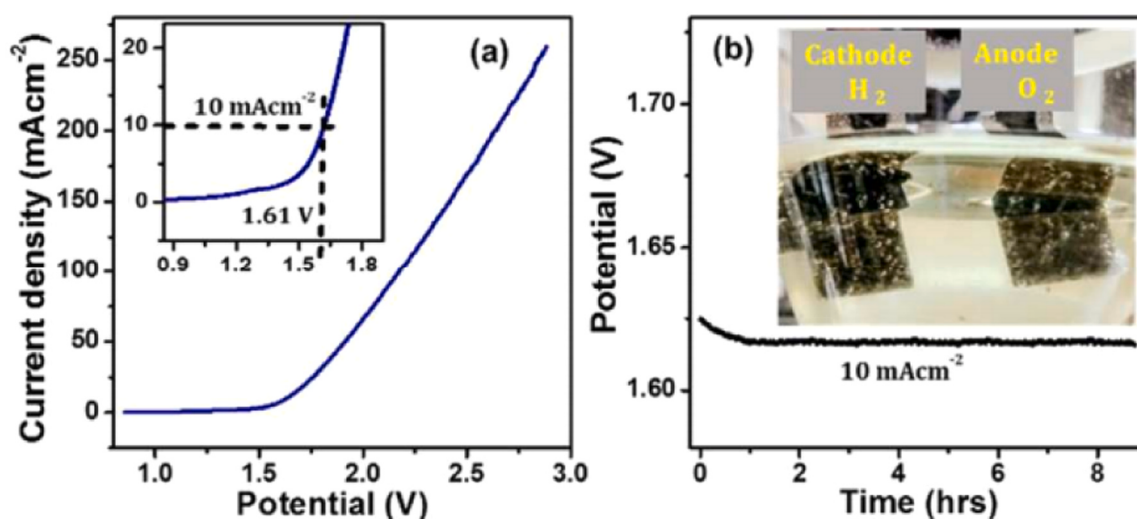


Fig. 3. (a) LSV polarization curve of water splitting in 1 M KOH at a scan rate of 5 mV s^{-1} using $\text{Co}_{0.4}\text{Fe}_{0.6}$, LDH)/g-CN_x as a cathode as well anode. Inset: Indicating potential required for 10 mA cm^{-2} (b) Chronopotentiometry response of $\text{Co}_{0.4}\text{Fe}_{0.6}$, LDH)/g-CN_x at 10 mA cm^{-2} . Inset: Photography of cathode and anode. Reprinted with permission from [63]. Copyright (2018), American Chemical Society.

maintain a stable catalytic current over 24 h without significant loss. Overall, a novel pathway could be developed to convert low-value biomass like fish scales into high-value materials using this method of preparing the Ni-Mo₂C/NC composite.

Furthermore, an electrocatalyst developed by amalgamating cobalt iron layered double hydroxide (Co_{0.4}Fe_{0.6} LDH) with g-CN_x using a one-pot co-precipitation followed by in-situ nucleation techniques [63]. The electrochemical performance of the Co_{0.4}Fe_{0.6} LDH/g-CN_x electrocatalyst for water-splitting reactions revealed a required potential of 1.61 V at an applied current density of 10 mA cm⁻² (Fig. 3a). Moreover, when testing the stability of the Co_{0.4}Fe_{0.6} LDH/g-CN_x composite, only slight changes in its potential value were observed after 9 hrs operational time (Fig. 3b). These results clearly demonstrated that the Co_{0.4}Fe_{0.6} LDH/g-CN_x composite has promising potential for efficient water splitting in alkaline conditions. A “bottom-up” self-assembled method was used for the development of a carbon-rich graphitic carbon nitride (CN) electrocatalyst using melamine and 2-hydroxypropyl-β-cyclodextrin (HC) as precursors (Fig. 4a) [64]. The developed CN electrocatalysts exhibit a larger surface-to-volume ratio and excellent light harvesting ability with much higher photocatalytic activity for hydrogen generation (Fig. 4b).

2.3. Transition metal oxides (TMOs) based composite materials

Nowadays, precious metals such as Ir, Ru, and Pt have demonstrated excellent electrochemical performance in terms of efficiency, activity, product selectivity, and cyclic stability in energy applications. However, due to their high cost and scarcity, their commercial usage is significantly limited [65–67]. On the other hand, transition metal oxide (TMOs)-based electrocatalysts exhibit a range of ideal properties, such as ease of preparation, high theoretical specific capacity, abundant sources, high storage capacity, and an environmentally friendly nature [68–70]. Several methods have been developed to enhance the electrocatalytic performances of TMO-based materials, as discussed in the literature [71]. These types of TMO-based electrocatalysts have recently emerged as potential candidates for the photoelectrochemical water-splitting process [72].

Using the co-precipitation technique, Shaghaghi et al. developed a heterofunctional cerium oxide-based copper oxide-supported cobalt oxide hybrid composite (CeO₂/CuO/Co₃O₄) [73]. The resulting CeO₂/CuO/Co₃O₄ heterostructured electrocatalysts exhibited excellent catalytic activity for both OER and HER under alkaline conditions. Specifically, they demonstrated a favorable potential value of 110 mV for HER and 520 mV for OER at an applied current density of 10 mA cm⁻² and these potential values are very low when compared to CeO₂/CuO and single CeO₂. Overall, the catalysts showed enhanced electron transport, high durability, and low charging current, as

evidenced by the characteristics of the Tafel slope and Nyquist plots. A low-cost, non-precious metal-based metal oxide-modified carbon heterogeneous crystalline composite (Fe/MnO@C) was developed using direct-current arc plasma strategies for OER application [74]. The Fe/MnO@C crystalline composite demonstrated a spin-pinning effect that reduces the kinetic barrier of OER studies. The synergistic effect within the crystalline composite rapidly enhanced the water-splitting process. Recently, the nanosheet morphology of FeO_x grown on nickel foam (FeO_x/NF) was achieved via an electrochemical method and optimized through a Li-ion induced conversion reaction method [75]. In addition, iron atoms in the tetrahedral arrangement influence the coordination of Fe in the octahedral configuration, thereby reducing Gibbs free energy and creating more catalytically active sites to accelerate rate-determining reactions. Ultimately, the FeO_x/NF-Li electrode facilitated the water-splitting reaction, demonstrating favorable potentials of 239 mV for HER and 276 mV for OER, respectively.

A novel in-situ electrochemical technique was employed to fabricate a composite of TMOs on conductive carbon fiber cloth (TMOs/CFC) [76]. Subsequently, this composite was transformed into transition metal sulfides (TMS) through a sulfurization process at 500 °C. Following this, the TMSs were electrochemically oxidized under alkaline conditions, reverting back to the crystalline nature of TMOs (Fig. 5). The as-synthesized electrochemically oxidized ECT-Co_{0.37}Ni_{0.26}Fe_{0.37}O electrode catalyst exhibited a low overpotential of 232 mV, a Tafel slope of 37.6 mV dec⁻¹, and demonstrated long-term stability within the water-splitting system.

Su et al. synthesized multi-shaped copper oxide nanoparticles (cuboctahedral, truncated cubic, octahedral, and truncated octahedral shapes) incorporated with MnO-MnO₂ nanorods [77]. These nanoparticles were dip-coated onto few-layer graphene and ITO substrates using a hydrothermal process followed by drop-coating techniques. The resulting Cu₂O/MnO-MnO₂ heterojunction photoelectrocatalyst was employed for hydrogen production via water splitting under solar radiation, achieving a rate of approximately 33.0 ml/min*m² (Fig. 6a). The electrochemical performance of the Cu₂O/MnO-MnO₂ photocatalyst was evaluated in 0.1 M KHCO₃ under dark field conditions. Throughout the photoelectrochemical water-splitting process, the maximum efficiency was observed at a bias voltage of 0.6 V (Fig. 6b).

2.4. Metal nanosheet (MNS) based composite materials

Electrode materials composed of nanosheets offer distinct benefits due to their abundant unsaturated sites, remarkable electrical conductivity, and distinctive characteristics stemming from their anisotropic attributes and the quantum confinement phenomenon. Nanosheets, as 2D nanostructures measuring between 1 and 100 nm in thickness, offer distinct benefits. These advantages include minimal solid-state ion

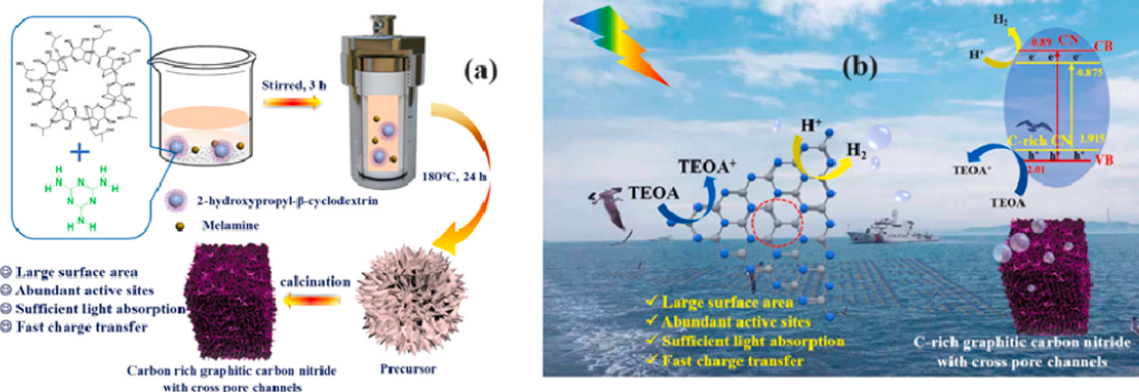


Fig. 4. (a) Synthesis route of carbon-rich graphitic carbon nitride with cross pore channels and (b) Proposed reaction mechanism for photocatalytic H₂ evolution on C-rich carbon nitride. Reprinted with permission from [64]. Copyright (2021), American Chemical Society.

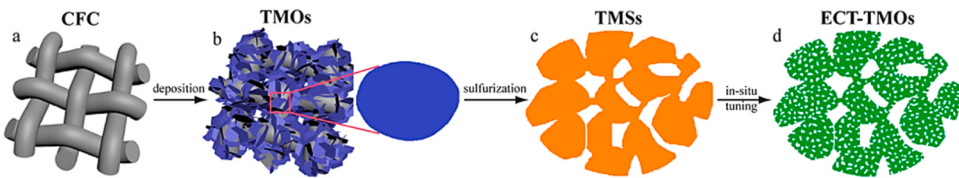


Fig. 5. Schematic representation of the synthesis process of ECT-TMOs and their corresponding morphology. (a) Carbon fiber cloth substrate. (b) Pristine TMOs were coated on CFC by one-step electrochemical deposition. (c) TMSs were obtained by the sulfurization treatment of the pristine TMOs. (d) ECT-TMOs formed by the in-situ electrochemical oxidation tuning of TMSs. Reprinted with permission from [76]. Copyright (2015), American Chemical Society.

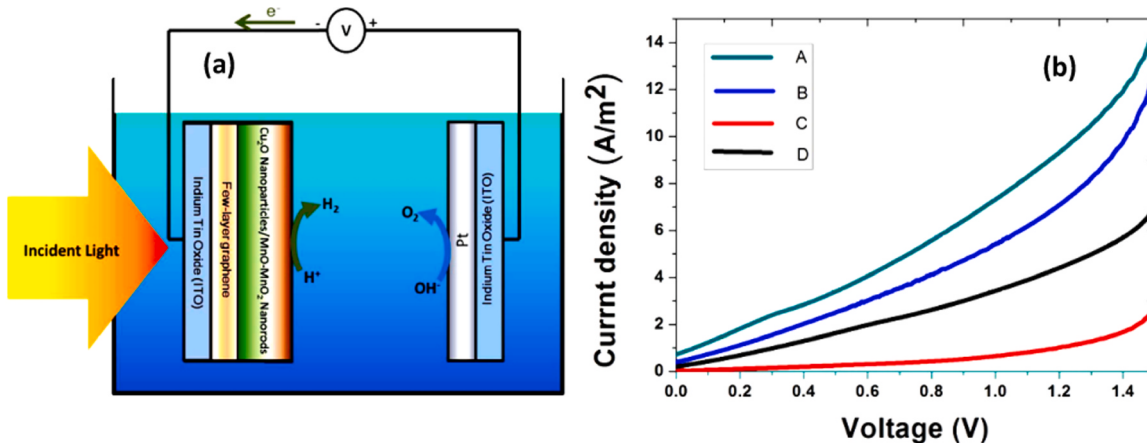


Fig. 6. (a) Scheme of the photovoltaic cell of water splitting under AM 1.5 G radiation and (b) Photoelectric current of multi-shaped Cu₂O nanoparticles on MnO nanorod supported by few-layer graphene on the ITO glass substrate (photocathode) in 0.1 M KHCO₃ under AM 1.5 G radiation. (Black line: truncated cubic, Red line: cuboctahedral, Blue line: truncated octahedral, Green line: octahedral). Reprinted with permission from [77]. Copyright (2015), American Chemical Society.

diffusion length, which benefits metal ions, effective improvement of electrode volume expansion during charge/discharge cycles, abundant channels facilitating swift ion diffusion within the electrode, and an embarrassment of active sites exposed for enhanced performance [78–80]. Consequently, nanosheet structures are highly esteemed as optimal electrode configurations for attaining superior energy storage capacity and rapid charge/discharge rates [81]. Moreover, there's been substantial interest in earth-abundant Ni-based catalysts, particularly the sheet-like configuration of nickel diselenide (NiSe₂), due to its inherent metallic traits, outstanding catalytic effectiveness, and strong chemical durability for HER activity in acidic environments [82]. Furthermore, recent research has highlighted the exceptional OER

electrocatalytic performance of Ni-based selenides in alkaline electrolytes, showing that manipulating morphology and employing doping modifications can further enhance their functionality [83]. Employing a facile two-step hydrothermal method, an orthorhombic-based NiSe₂ electrocatalyst has effectively grafted on carbon cloth. This resulting NiSe₂/CC structure, prepared in this manner, serves as flexible electrodes suitable for cathode and anode, displaying remarkable performance in overall water-splitting reactions [84].

The hydrothermal method was employed to create an effective ultrathin structure of graphdiyne-wrapped iron carbonate hydroxide nanosheets (FeCH@GDY/NF) through a two-step process [85]. The successful synthesis of these ultrathin FeCH nanosheets was confirmed

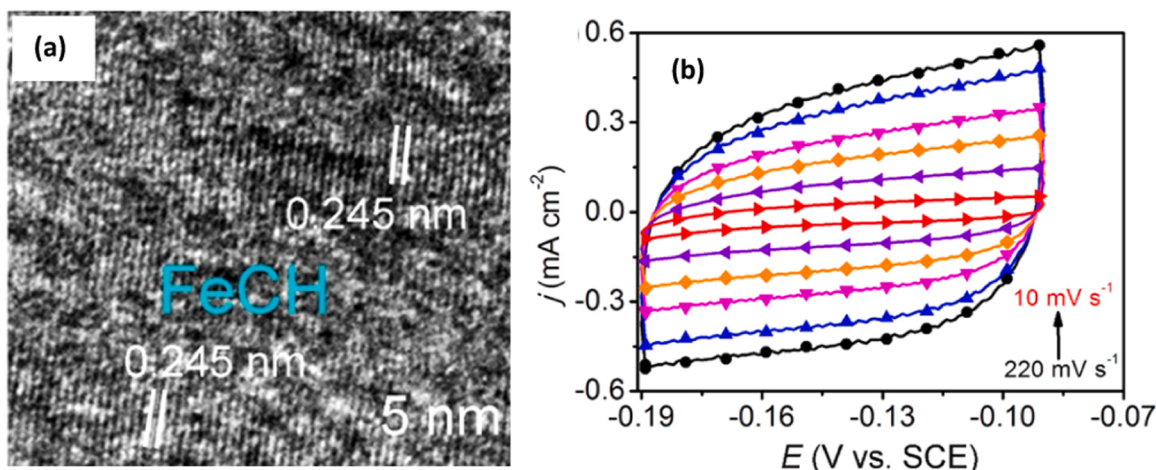


Fig. 7. (a) HR-TEM image of FeCH@GDY nanosheets and (b) Cyclic voltammograms of FeCH@GDY/NF at a scan rate of 10 mV s^{-1} . Reprinted with permission from [85]. Copyright (2019), American Chemical Society.

by the HR-TEM image, as depicted in Fig. 7a. Notably, the lattice fringe spacing of FeCH was measured at 0.245 nm. The as-developed FeCH@GDY/NF catalyst demonstrated a capacitance double layer value of 1.0 mF cm^{-2} . This value represents a substantial enhancement in the active surface area compared to both FeCH/NF (0.39 mF cm^{-2}) and GDY/NF (0.13 mF cm^{-2}), displaying an increase of approximately 2.6 and 7.7 fold, respectively. This outcome suggests a notable augmentation in the active surface area following the application of the thin GDY layer (Fig. 7b).

A simple approach was employed using carbonization and phosphorization to fabricate composite materials comprising 2D cobalt phosphide nanoparticles with N-doped carbon (Co-P@NC) (Fig. 8a) [86]. The electrocatalytic performance of Co@NC-800 and Co-P@NC-800 in a 1 M KOH solution is depicted in Fig. 8b. Notably, both Co@NC-800 and Co-P@NC-800 demonstrated favorable OER activities. Significantly, Co-P@NC-800 exhibited superior OER performance compared to Co@NC-800. Specifically, it achieved a current density of 10 mA cm^{-2} at an overpotential of 370 mV, whereas Co@NC-800 required 450 mV for the same current density. Despite the generation and sudden release of abundant O_2 gas bubbles from the electrode, which might potentially dislodge the catalyst, galvanostatic measurements at a current density of 10 mA cm^{-2} demonstrated that Co-P@NC-800 exhibited better electrode stability for a minimum of 6000 s (Fig. 8c).

2.5. Hexagonal boron nitride-based composite materials

Recently, there has been considerable interest in utilising hexagonal boron nitride (h-BN), categorized as a 2D material, within the promising material of green energy applications. The latest progressions in materials science and nanotechnology have brought to light compelling uses for h-BN, leveraging its distinct chemical and electrochemical attributes, remarkable thermal stability, expansive surface-to-volume ratio, favorable optical characteristics, and environmentally friendly nature [87–90]. These advancements have revealed promising avenues for h-BN beyond its conventional applications. Z-schemes utilizing

hexagonal-boron carbonitride (h-BCN) have demonstrated promise because of their effective separation of oxidation and reduction zones, sturdy capability to harness light, exceptional migration and separation of charge pairs, and impressive capability for redox reactions. As a metal-free photocatalyst, h-BCN has gained considerable attention in research circles owing to its adjustable band-gap spanning from 0 to 5.5 eV [91].

Wang and coworkers utilized a one-pot chemical vapor deposition method to grow h-BN on a graphene electrode [92]. This technique facilitated the epitaxial intercalation of graphene under a hydrogen-terminated hBN template, resulting in inter-layer angles converging to less than 0.5° . The stacking angle approaching 0° exhibited a significantly higher possibility of occurrence almost two orders of magnitude more compared to angles better than 0.5° . The resulting uniformly grown hBN/graphene bi-layer composite effectively controlled inter-layer rotation, holding promise for advancing the production of high-quality van der Waals (vdW) heterostructures. The durable nature of h-BN provides a sturdy foundation, preserving the structural stability of heterostructured catalysts. Both empirical observations and theoretical computations demonstrate that the potent interaction between h-BN and Pd induces a downward shift in the Pd d-band center, thereby enhancing its compatibility with reaction intermediates. This presents a novel pathway for strategically designing and advancing heterostructured catalysts through interface manipulation, particularly for electrocatalytic applications [93]. h-BN has garnered considerable interest owing to its analogous structure and characteristics compared to graphite, which has become a focus due to its 2D layered arrangement. Its application in catalytic reactions has been extensive.

For comparison, results from the bare NiFeO_xHy electrode are multiplied by nine times. Moreover, a composite, B-hBN-Ni P, incorporating h-BN, was utilized to enhance HER, leading to a substantial improvement in the rate of hydrogen evolution [94]. Significantly, h-BN-based heterojunction electrocatalysts have been widely applied in diverse electrochemical applications, spanning hydrogen energy storage [95], potassium ion batteries [96], and electrochemical sensors [97].

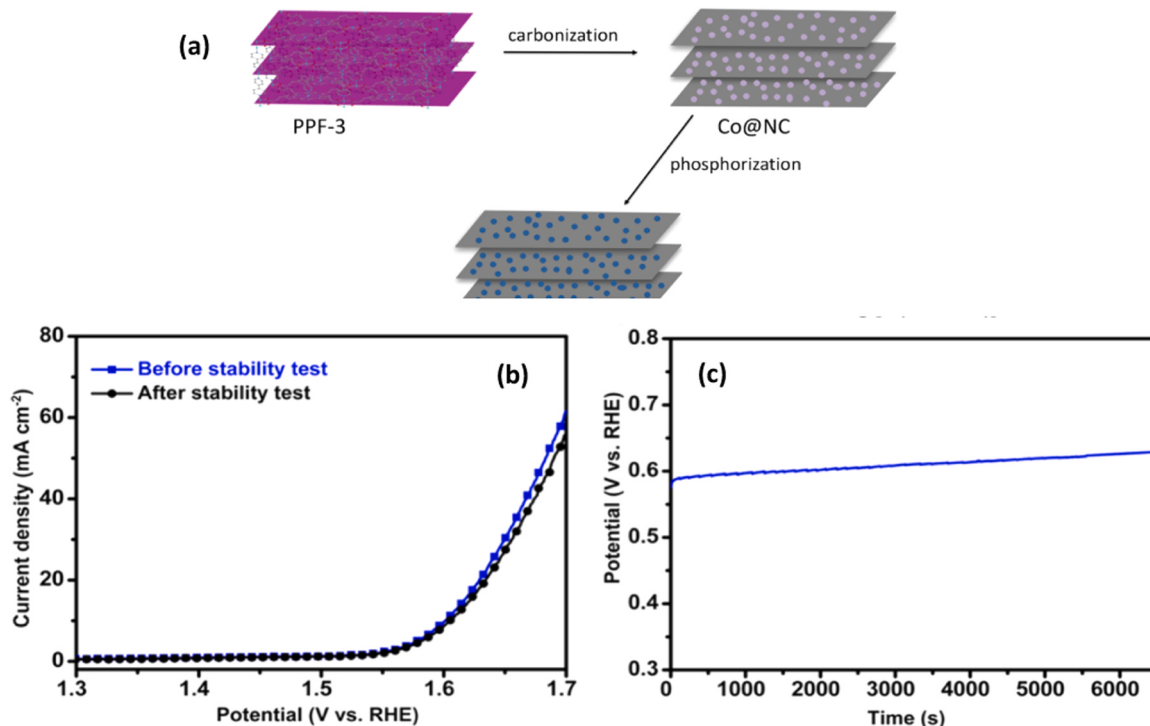


Fig. 8. (a) Preparation of Co-P@NC, (b) and (c) OER polarization curves of Co-P@NC-800 before and after the stability test at 10 mA cm^{-2} . Reprinted with permission from [86]. Copyright (2015), American Chemical Society.

Utilizing chemical vapor deposition, one-atom-thick hBN films were successfully synthesized on Cu substrates. These films encapsulate various electrocatalytic electrodes, forming centimeter-sized, impermeable hBN surfaces that exclusively expose themselves to reactive species.

In Fig. 9a, a typical current-voltage characteristic for the OER is depicted. At an overpotential (η) of 230 mV (where $\eta = \text{VRHE} - 1.23 \text{ V}$, the theoretical equilibrium potential for water electrolysis), the recorded current density (j) reaches 10 mA cm^{-2} , exhibiting a rapid increase with VRHE at a slope of nearly 30 mV dec^{-1} . Gas chromatography results (Fig. 9b) confirm the generation of O_2 and H_2 (in a molar ratio of 1:2) with a Faraday efficiency exceeding 99%. Crucially, our electrode demonstrates exceptional stability, maintaining a current variation of less than 10% even at $j = 2000 \text{ mA cm}^{-2}$ over 150 hours (Fig. 9c) [98].

2.6. Perovskite-based composite materials

Perovskites-based electrode materials, renowned for their cost-effectiveness, versatile structures, and inherent oxygen vacancy content, have emerged as key materials in numerous electronic applications and have experienced considerable attention and rapid growth [99–101]. A typical composition of perovskite materials follows the structure ABX_3 , marking their significance in the field. Perovskite oxide electrocatalysts, comprised of cations 'A' and 'B' along with the anion 'X', typically oxides or halogens, exhibit a distinctive structural arrangement. 'A' cations like calcium, lanthanum, lead, and strontium, larger than 'B' cations, occupy 12-fold oxygen-coordinated holes and possess lower valence states [102]. These electrocatalysts, particularly the perovskite oxide ($\text{ABO}_{3-\delta}$) variants, have garnered significant attention due to their inherent advantages, namely, compositional

flexibility and adaptable structure. The intriguing aspect lies in the considerable substitutions possible at the A, B, and O sites, enabling perovskite oxides to display exceptional flexibility in their redox-active sites and oxygen vacancy distribution. Consequently, these substitutions significantly influence the physicochemical properties and catalytic performance of these materials, making them highly promising for various catalytic applications [103,104].

The monoclinic based SrIrO_3 perovskite, a highly efficient alkaline electrocatalyst, shows excellent conductivity and simple synthesis protocol in standard conditions. During activation for the HER, the catalyst gradually undergoes surface self-reconstruction by leaching lattice Sr^{2+} ions, leading to an impressive 11-fold activity increase at 200 mV overpotential. Additionally, in a two-electrode water-splitting system, the SrIrO_3 -based cell achieves exceptional performance, attaining 1.59 V at 10 mA cm^{-2} and sustaining minimal degradation over 10 h [105]. A simple and cost-effective anodization technique and a continuous roll-to-roll process are utilized to create an enhanced $\text{NiFe}(\text{oxy})$ hydroxide electrocatalyst. The synthesized catalyst demonstrates significantly improved performance, exhibiting an overpotential of 250 mV at 10 mA cm^{-2} , notably lower than the bare NiFe alloy's overpotential of 380 mV at 10 mA cm^{-2} . Leveraging cost-effective solution-based methods, the photovoltaic–electrocatalysis (PV-EC) system outperforms the latest high-efficiency solar water splitting systems, presenting distinct advantages [106]. Further, Xiaoqin Sun *et al.* developed Sr_2TiO_4 of the Ruddlesden-Popper (RP) type and introduced co-doping of La/N into this layered perovskite [107]. The unmodified Sr_2TiO_4 does not show any catalytic response to HER and OER due to its wide band gap nature, thereby no sensitive to visible light photons. However, the incorporation of La/N through co-doping was found to broaden the light absorption capabilities of Sr_2TiO_4 , extending it up to

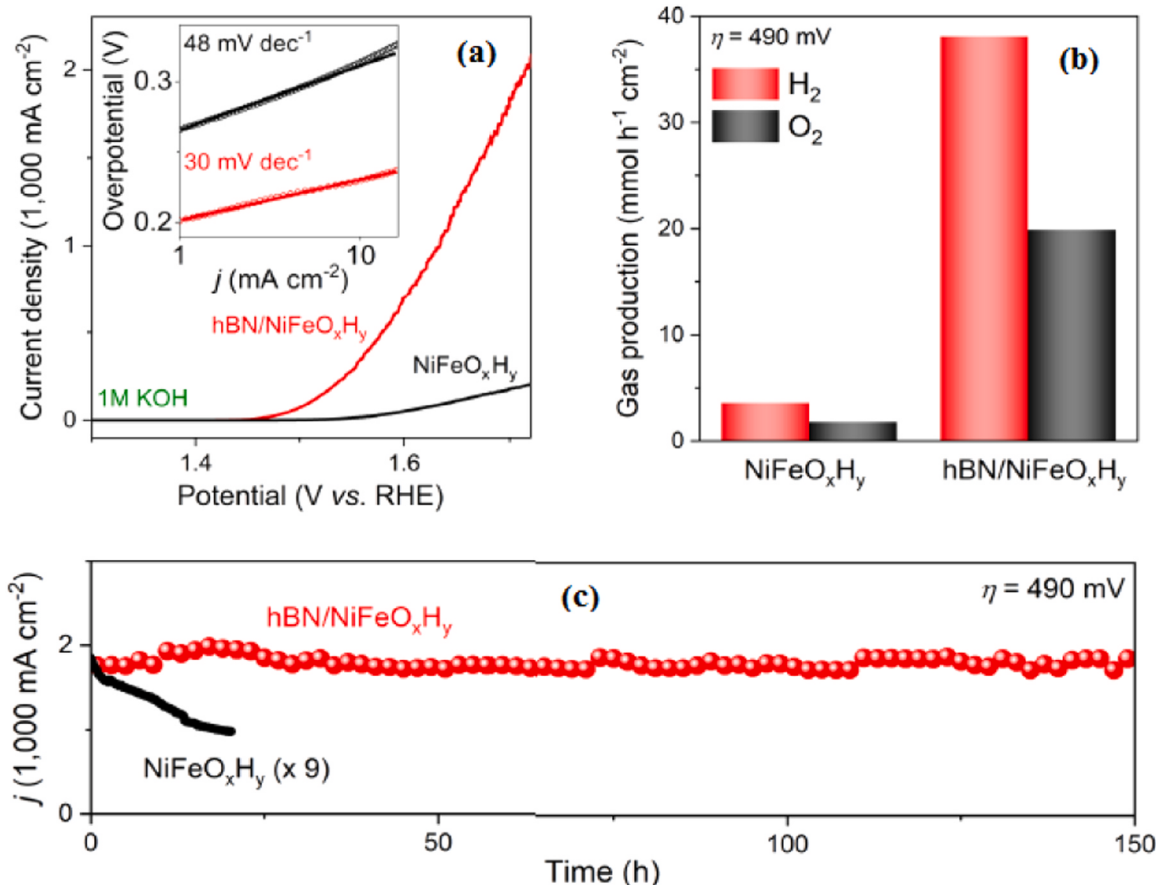


Fig. 9. (a) Linear sweep voltammetry (Inset: Tafel slopes), (b) Gas product analysis at $\eta = 490 \text{ mV}$ and (c) Stability of bare NiFeO_xH_y and hBN/ NiFeO_xH_y electrodes. Reprinted with permission from [98]. Copyright (2023), American Chemical Society.

650 nm. This alteration resulted in significantly enhanced visible-light-driven photocatalytic efficacy for the process of water splitting. To promote the photo-reduction/oxidation process, sodium sulfite or silver nitrate was added as a sacrificial agent. Also, 1% of Pt or CoOx was incorporated with the Sr₂TiO₄ to further improve the HER and OER responses.

A nanoporous structure, achieved through hydrothermal conversion of TiO₂ nanoporous film, transformed it into a non-metallic plasmonic SrTiO₃ photoelectrode. Following this, a reduction treatment was applied. Displayed in Fig. 10a is the HR-TEM image of r-SrTiO₃, revealing the presence of a visibly disordered layer measuring approximately 4 nm in thickness on its surface. Furthermore, the core of r-SrTiO₃ maintains a high degree of crystallinity, as evidenced by a measured lattice spacing of 0.27 nm, aligning with the characteristic cubic SrTiO₃ (110) plane. This observation, verified by HR-TEM analysis, reaffirms the crystalline core@amorphous-shell configuration of the nanoporous film in r-SrTiO₃. As depicted in Fig. 10b, the mechanism illustrating the LSPR effect of r-SrTiO₃ in the photoelectrochemical (PEC) splitting of water involves the plasmonic SrTiO₃ disordered shell functioning as a photosensitizer under visible light, capturing resonant photons. The LSPR-induced energetic hot electron-hole pairs facilitate the transfer of hot electrons to the conduction band of the neighboring crystalline SrTiO₃ core. These electrons then travel through an external circuit to the counter electrode (Pt photocathode) to initiate the water reduction reaction (Fig. 10c) [108].

A double perovskite oxide photocatalyst, Sr₂CoTaO₆, exhibiting visible-light absorption, was successfully synthesized using a flux-

assisted method. This method involved annealing at a relatively low temperature of 900 °C for a short duration of 15 hours, resulting in the creation of Sr₂CoTaO₆-F. To evaluate its efficacy, Sr₂CoTaO₆-F was compared with Sr₂CoTaO₆ synthesized via the conventional solid-state reaction method, denoted as Sr₂CoTaO₆-S, which underwent annealing at a higher temperature of 1150 °C for 5 days. Sr₂CoTaO₆-F displayed significantly enhanced photocatalytic capabilities in both the OER and HER when compared to Sr₂CoTaO₆-S. This contrast highlights the advantageous control over crystallinity and morphology achieved through the flux method in synthesizing double perovskite oxides. Notably, Sr₂CoTaO₆-F exhibited remarkable bifunctional OER and HER activities without additional cocatalysts being needed [109].

2.7. MXene-based composite materials

MXene-based electrocatalysts, composed of transition metal carbides and nitrides, have garnered significant attention in various critical research domains. Their utilization has become widespread due to several advantageous characteristics, such as substantial surface areas, high mobility and energy densities, exceptional mechanical robustness, superior electrical conductivity, customizable surface chemistry from transition metal surfaces, and effortless dispersion across diverse solvents [110–113]. MXene-based materials, prominent for their excellent electrochemical properties and superior conductivity, have found extensive application as superior electrode materials in supercapacitors [114], sodium-ion batteries [115], and Li-S batteries [116] due to their exceptional attributes. Over the past two decades, there has been

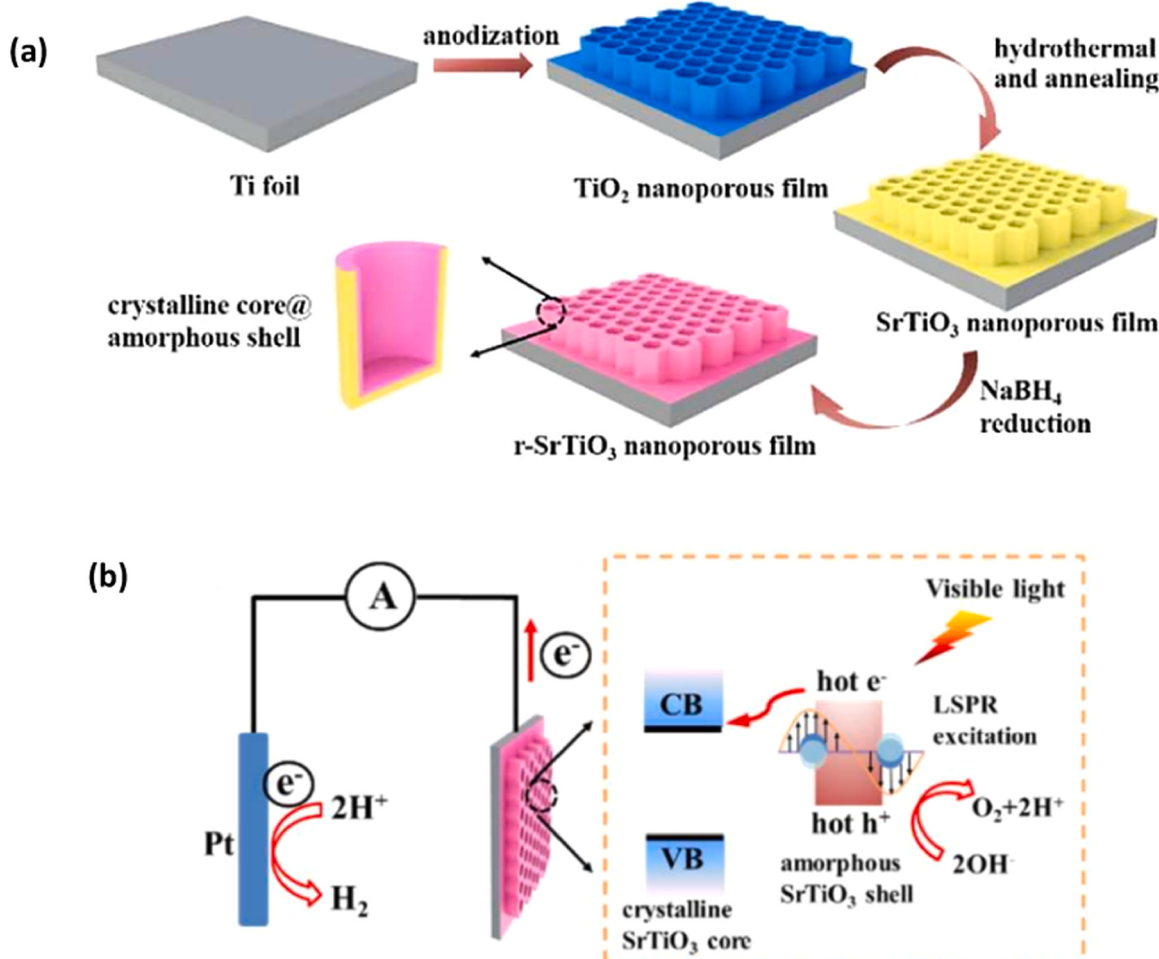


Fig. 10. (a) Schematic illustration of the preparation of r-SrTiO₃ and (b) Proposed mechanism of r-SrTiO₃ for PEC splitting under visible light. Reprinted with permission from [108]. Copyright (2018), American Chemical Society.

substantial exploration into the potential utilization of Mxene materials in the field of water-splitting reactions. These materials, characterized as 2D nanomaterials, have gained extensive attention due to their composition involving covalent bonds between transition elements and carbon [117,118].

2D layered MXene-based electrocatalysts have been developed through various routes, including self-assembly [119,120] and in-situ precipitation [121] techniques. For instance, Xie *et al.* successfully grafted a semiconductor photoelectrode composed of MXene-based ZnO_2 nanorod arrays, generating significant interest for practical applications in PEC water-splitting reactions [122]. The system will thereby stabilize due to physical adsorption, inducing interlayer self-accumulation through the force of van der Waals. Consequently, the ZnO /MXene photoanode exhibited a remarkable enhancement in its performance for PEC water splitting. The emergence of cost-effective and highly efficient noble metal-free Ti_3C_2 MXene-based electrocatalysts through a facile synthesis route is noteworthy. These promising electrocatalysts have demonstrated enhanced performance in both the HER and OER activities. The observed improvement in TC40 MXene's performance can be attributed to its abundant active sites and remarkable charge transfer capability. Furthermore, TC40 MXene underwent evaluation as a bifunctional electrocatalyst for complete water splitting [123]. Furthermore, Li *et al.* employed both experimental and theoretical methodologies to explore the water-splitting capabilities of FeCo-layered double hydroxide and $P-MoO_3$, grown using an in-situ technique on MXene [124]. This catalyst, prepared in such a manner, exhibited exceptional catalytic activity in enabling overall water splitting, achieving a current density of 10 mA cm^{-2} with minimal

overpotentials of 179 mV for OER and 118 mV for HER. Additionally, the corresponding Tafel slopes were notably low, registering at $40.44 \text{ mV dec}^{-1}$ for OER and 105 mV dec^{-1} for HER, signifying an enhanced kinetic performance. In addition, the hybrid films consisting of binder-free CTAB-rGO-modified MXene-based electrode materials were created using layer-by-layer assembly and dip coating techniques applied on nickel foam [125]. These films represent a promising substitute for noble metal-based electrodes. These electrodes exhibited enhanced catalytic activity for electrochemical water splitting. The as-synthesized CTAB-rGO-modified MXene hybrid electrode demonstrated considerable performance enhancements, showcasing a current density of 10 mA/cm^2 at an overpotential (η) of 360 mV and a Tafel slope value of 56.6 mV/dec for the HER. Similarly, in an alkaline medium, the OER exhibited a current density value of 10 mA/cm^2 at an overpotential (η) of 179 mV, along with a Tafel slope value of 47.03 mV/dec .

The exfoliated Ti_3C_2 MXenes were utilized as a substrate to vertically grow uniformly mesoporous NiCoP nanosheets employing an in-situ interface-growth approach, followed by phosphorization (Fig. 11a) [126]. Examination of the cross-section revealed clearly identifiable sandwiched $Ti_3C_2@NiCo_2O_4$ NSs. TEM image unveiled that the ultrathin Ni-Co nanosheets grown on the surface measure approximately 4 nm in thickness, exhibiting abundant, visibly uniform mesopores. These interconnected ultrathin porous nanosheets are evidently conducive to enhancing mass transport during electrocatalysis. HR-TEM image depicted lattice fringes of the composite (Fig. 11b). The $Ti_3C_2@mNiCoP$ NS demonstrates substantial promise as a bifunctional electrocatalyst for water-splitting in alkaline electrolyte. To assess the water-splitting

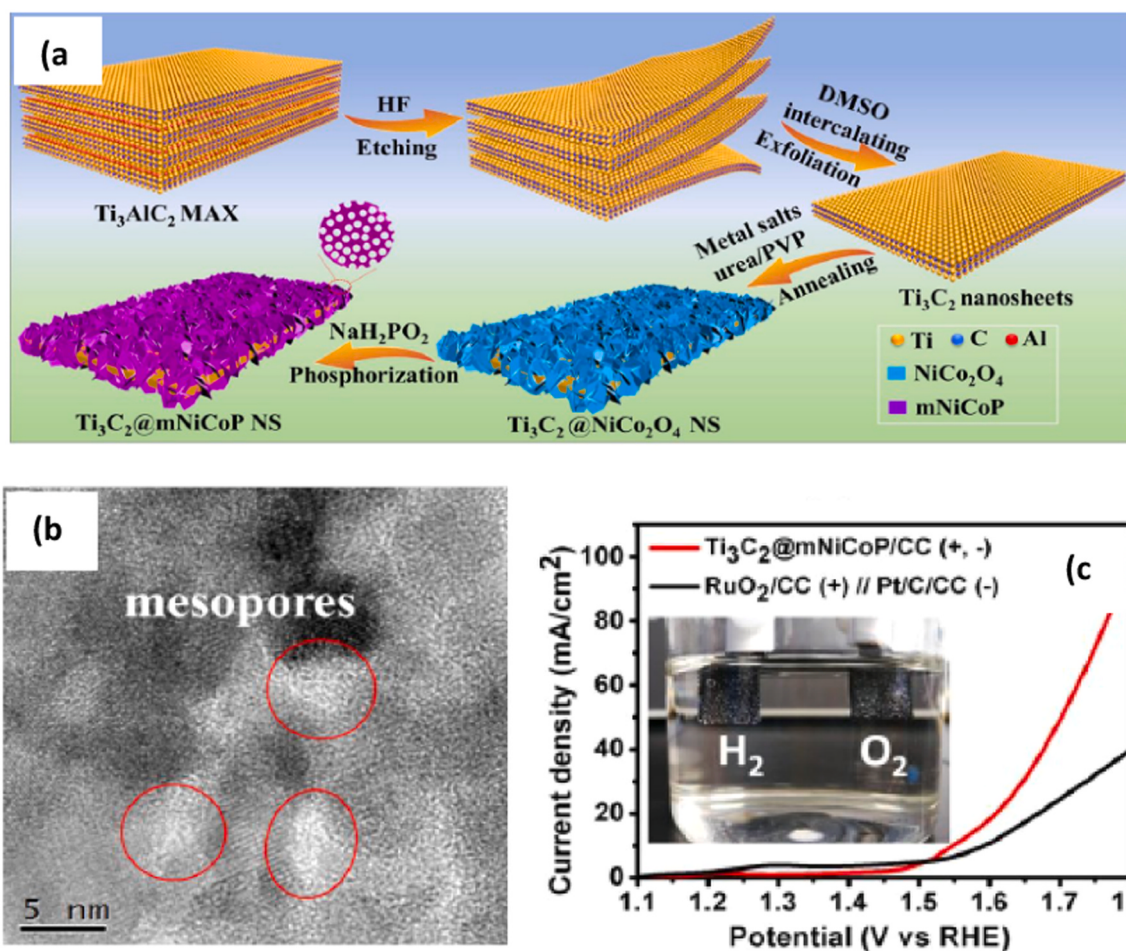


Fig. 11. (a) Schematic illustration of the synthesis of hierarchical $Ti_3C_2@mNiCoP$ NS, (b) TEM image of $Ti_3C_2@mNiCoP$ nanosheets and (c) Electrocatalytic water-splitting of developed electrodes in an alkaline medium. Reprinted with permission from [126]. Copyright (2020), American Chemical Society.

performance, $\text{Ti}_3\text{C}_2@\text{mNiCoP}$ NSs were applied to CC with a mass loading of 2.0 mg cm^{-2} for both electrodes and evaluated in a two-electrode cell. As illustrated in Fig. 11c, the steady-state polarization curve indicates that a cell voltage of 1.57 V and 1.70 V is necessary to achieve a current density of 10 mA cm^{-2} and 50 mA cm^{-2} , respectively [126].

A hydrothermal method was used to develop core-shell MXene@Carbon Nanodots (Fig. 12a) [127]. The morphological analysis of both the pristine and core-shell structures was conducted via HR-TEM (Fig. 12b), revealing an average thickness of 1.6 nm for the core-shell. To compare the PEC performance, $\text{MX}@C/\text{BVO}(-)\|\text{MX}@C$ was tested on Ni foam(+) cells against a $\text{BVO}(-)\|\text{Ni foam}(+)$ cell. As illustrated in the J-V curves obtained from the LSV mode in Fig. 12c, the Ni foam-based PEC cell featuring $\text{MX}@C/\text{BVO}\|\text{MX}@C$ attained a current density of 1.23 mA/cm^2 at 1.23 V , marking a 157% increase compared to the 0.78 mA/cm^2 achieved by the $\text{BVO}\|\text{Ni foam}$ cell.

2.8. Layered double hydroxides (LDHs) based composite materials

Layered double hydroxides (LDHs) have garnered increased attention in electrochemical energy storage and conversion owing to their 2D nature. These materials, considered typical in the realm of 2D materials, exhibit substantial promise in this field due to their adaptable composition, structure, and morphology through various preparative methodologies. They belong to the captivating category of inorganic materials that offer adjustable chemical composition and structures, often recognized as anionic clays or hydrotalcite.

Comprising positively charged layers of metal hydroxides alongside charge-balancing anions and water molecules between the layers, LDHs

are denoted by the general formula $[\text{M}_{1-x}^{2+}\text{M}^{3+}x(\text{OH})_2]^{+}(\text{A}^{n-})_{x/n}\cdot\text{mH}_2\text{O}$, wherein M^{2+} and M^{3+} refer to di- and trivalent metal cations, respectively, while A^{n-} represents the interlayer guest ions having an n -valence [128–130]. Ongoing advancements in fabrication techniques are broadening the potential application range of LDHs as electrode materials across various electrochemical domains, including supercapacitors [131], sodium-ion batteries [132], lithium-ion batteries [133], and solar cells [134] applications. These developments aim to harness the distinct qualities of LDHs, enhancing their versatility and effectiveness in a wider array of electrochemical applications.

Investigations into the water-splitting reaction have recently focused on the performance of 2D layered oxides and hydroxides possessing edge-sharing octahedral structures (MO_6) [135]. Zhang *et al.* employed a hydrothermal approach to craft nanostructures composed of silver nanowire@nickel–iron LDH (Fig. 13a) [136]. The observed improvement in catalytic performance stems from swift electron transfer to the active centers and a synergistic effect facilitated by the presence of Ag and its oxidized state. Additionally, the commendable stability arises from the enduring nature of Ag NWs in alkaline settings. Fig. 13b illustrates the corresponding LSVs. Notably, the Ag NWs@ $\text{Ni}_{0.95}\text{Fe}_{0.05}$ LDHs curve demonstrates electrocatalytic water splitting at a current density of 10 mA cm^{-2} , achievable under a remarkably low potential of 1.7 V . This achievement represents an outstanding 62% energy efficiency compared to the theoretical value at 1.23 V .

Through a hydrothermal process, a self-supported electrocatalyst comprising NiFe LDH-NiSe, was developed via gradual surface-redox-etching of Ni foam (NF). This innovative NiFe LDH-NiSe/NF catalyst demonstrates superior performance in alkaline water oxidation, proton reduction, and overall water splitting compared to NiSex/NF or NiFe

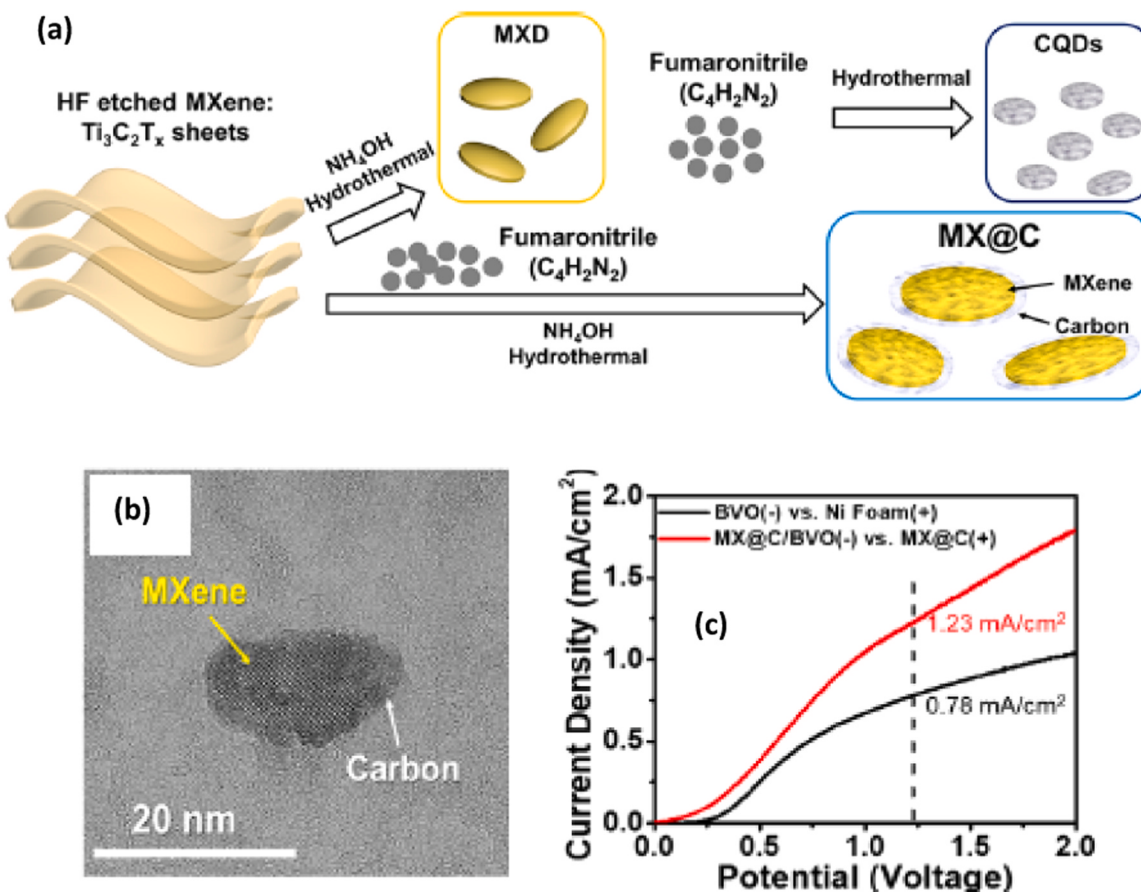


Fig. 12. (a) Schematic illustration of the synthesis of MXDs, (b) HR-TEM image of MX@C and (c) J-V curves of solar-assisted overall water splitting cells under AM 1.5 G sun illumination of $\text{BVO}(-)$ vs Ni foam(+) and $\text{MX}@C/\text{BVO}(-)$ vs $\text{MX}@C(+)$ (on Ni foam, +). Reprinted with permission from [127]. Copyright (2020), American Chemical Society.

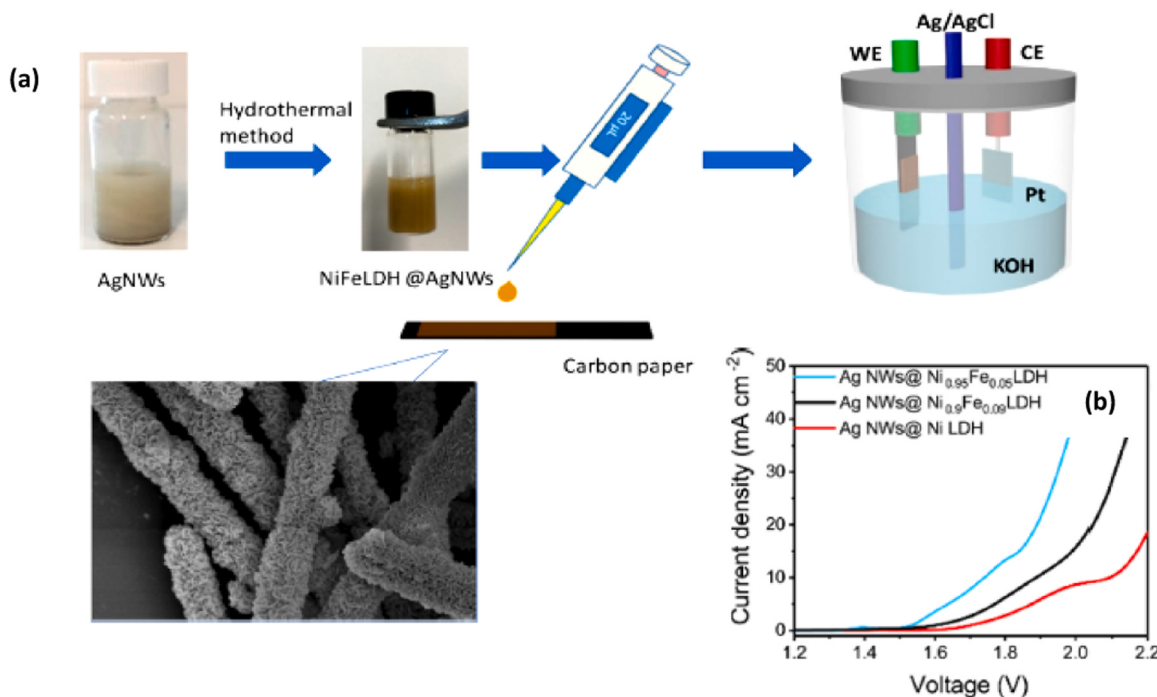


Fig. 13. (a) Schematic illustration of the synthetic process for the Ag@NiFe LDH and (b) LSV curve of overall water splitting. Reprinted with permission from [136]. Copyright (2020), American Chemical Society.

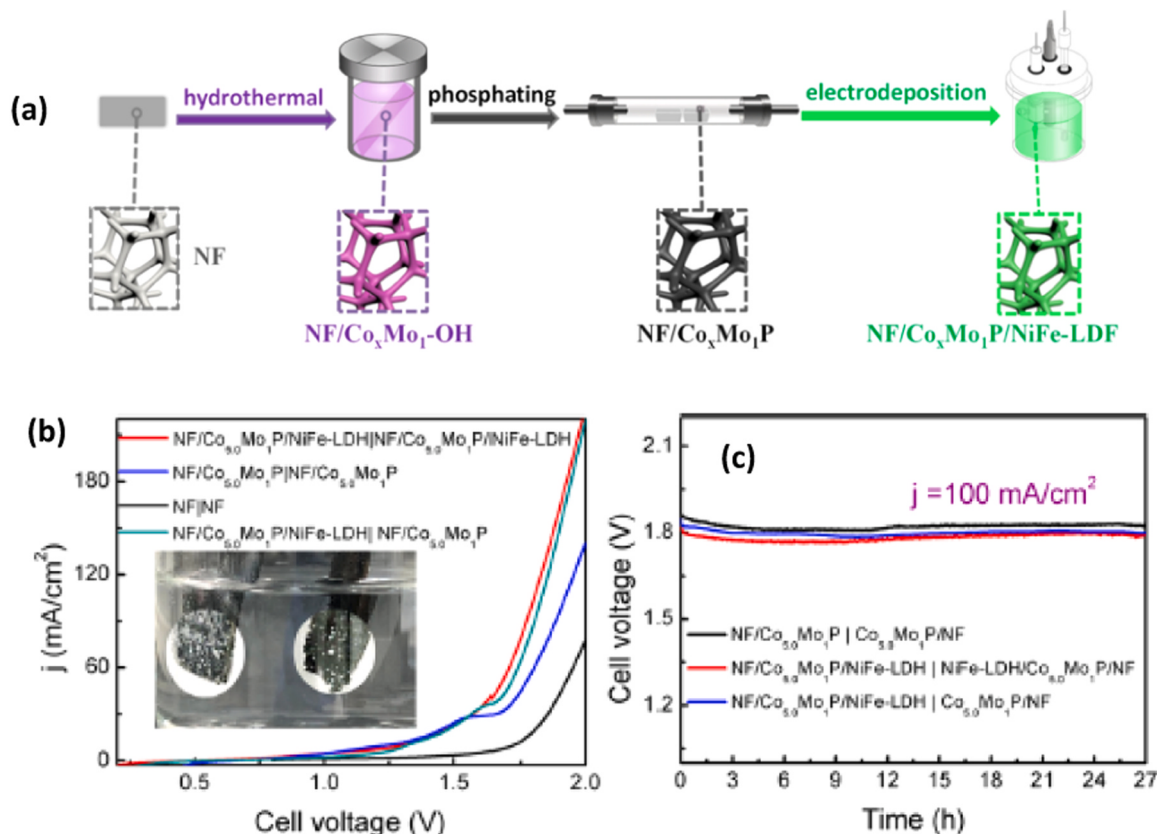


Fig. 14. (a) Schematic representation of the preparation of Co_xMo₁P/NiFe-LDH on the NF substrate, (b) OWS polarization curves of NF/Co_{5.0}Mo₁P/NiFe-LDH|NiFe-LDH/Co_{5.0}Mo₁P/NF, NF/Co_{5.0}Mo₁P/NiFe-LDH|Co_{5.0}Mo₁P/NF, NF/Co_{5.0}Mo₁P|Co_{5.0}Mo₁P/NF, and NF|NF cells at 5 mV/s and (c) Operational stability tests carried out at constant current densities of 100 mA/cm². Inset is the digital photograph of the single-electrolyte cell with two electrodes. Reprinted with permission from [141]. Copyright (2020), American Chemical Society.

LDH/NF. Achieving a water oxidation current density of 100 mA cm^{-2} demands only a 240 mV overpotential, while for the HER, the requirement stands at 276 mV in 1.0 M KOH [137]. Using a distinct Ostwald ripening driven exfoliation (ORDE) technique, NiFe LDHs are exfoliated in situ directly on electrodes. This spontaneous process occurs during a straightforward hydrothermal treatment, removing the necessity for exfoliating agents or surfactants. Consequently, this yields ultrathin, clean, vertically aligned NiFe nanosheets with an expanded surface area, abundant exposed active edges, and sites. These nanosheets demonstrate improved OER performance, with a low overpotential of 292 mV at 10 mA cm^{-2} , exceptional stability exceeding 60 hours, and remarkable flexibility [138].

The in-situ technique was used in the development of low-level Fe-doped Ni-layered double hydroxide ($\text{Ni}_{1-x}\text{Fe}_x\text{-LDH}$) and Co-layered double hydroxide ($\text{Co}_{1-x}\text{Fe}_x\text{-LDH}$) in a layer-by-layer fashion. To assess the overall water-splitting performance of these electrocatalysts as both anode and cathode, three variations of alkaline electrolyzers were constructed: $\text{Co}_{1-x}\text{Fe}_x\text{-LDH}(+)\parallel\text{Co}_{1-x}\text{Fe}_x\text{-LDH}(-)$, $\text{Ni}_{1-x}\text{Fe}_x\text{-LDH}(+)\parallel\text{Ni}_{1-x}\text{Fe}_x\text{-LDH}(-)$ and $\text{Co}_{1-x}\text{Fe}_x\text{-LDH}(+)\parallel\text{Ni}_{1-x}\text{Fe}_x\text{-LDH}(-)$. Remarkably, these electrolyzers exhibit efficiency with a minimal cell potential (E_{cell}) requirement of 1.60, 1.60, and 1.59 V, respectively, to achieve a benchmark current density of 10 mA cm^{-2} [139]. On the other hand, Wu *et al.* developed a structured array of nanosheets consisting of NiFe_2O_4 nanoparticles/NiFe LDH on Ni foam using a one-step solvothermal method [140]. This particular configuration exhibits outstanding overall water-splitting capabilities by employing NiFe_2O_4 nanoparticles/NiFe LDH nanosheets as both anode and cathode, continuously powered by just a 1.5 V battery. The synergistic effects between NiFe_2O_4 nanoparticles and NiFe LDH nanosheets create numerous catalytically active sites, ensuring high electronic conductivity and exceptional catalytic reactivity for OER and HER and the overall water splitting process.

A 3D porous electrode assembly was constructed using a 2D heterostructure, where NiFe-LDH nanosheet arrays were electrodeposited vertically onto the surface of bimetallic nanoflowers. These bimetallic nanoflowers were previously generated on the NF substrate through a hydrothermal–phosphating process, forming a structured assembly (Fig. 14a). The enhanced performance can be attributed to the extensive exposure of active sites facilitated by the 2D porous and hierarchical nanosheet arrays, along with efficient electronic coupling and rapid electronic transmission across diverse interfaces. Electrochemical assessments revealed that $\text{NF}/\text{Co}_{5.0}\text{Mo}_{1.0}\text{P}/\text{NiFe-LDH}$ demonstrates not only exceptional performance for both HER and OER, showcasing an HER overpotential (η at 10 mA/cm^2) of 98.9 mV and an OER overpotential (at 50 mA/cm^2) of 225 mV, surpassing $\text{NF}/\text{Co}_{5.0}\text{Mo}_{1.0}\text{P}$ and NF/CoP , but also exhibits remarkable stability in 1.0 M KOH (Fig. 14b). Additionally, it achieves a cell voltage of 1.68 V for water splitting at 50 mA/cm^2 , demonstrating excellent durability for over 27 hours (Fig. 14c) [141]. Further, Liang *et al.* prepared a heterostructural nickel-cobalt phosphide-based bimetallic LDH on nickel foam (NiCoP@NiMn LDH/NF) bifunctional electrocatalyst using a facile hydrothermal process (Fig. 15a) [142]. The constructed heterostructured array of NiCoP@NiMn LDH/NF exhibits significantly enhanced water-splitting activity compared to previously reported electrocatalysts under alkaline conditions, as depicted in Fig. 15b.

2.9. Metal chalcogenides (MCs) based composite materials

"Platinum group-based metals (PGMs) such as rhodium, platinum, iridium, and palladium have long been utilized as highly efficient electrocatalysts in the commercial water-splitting process [143]. However, these noble electrocatalysts derived from PGMs are rare and exceedingly expensive, and their scarcity poses negative environmental impacts, rendering the commercial water electrolyzer process

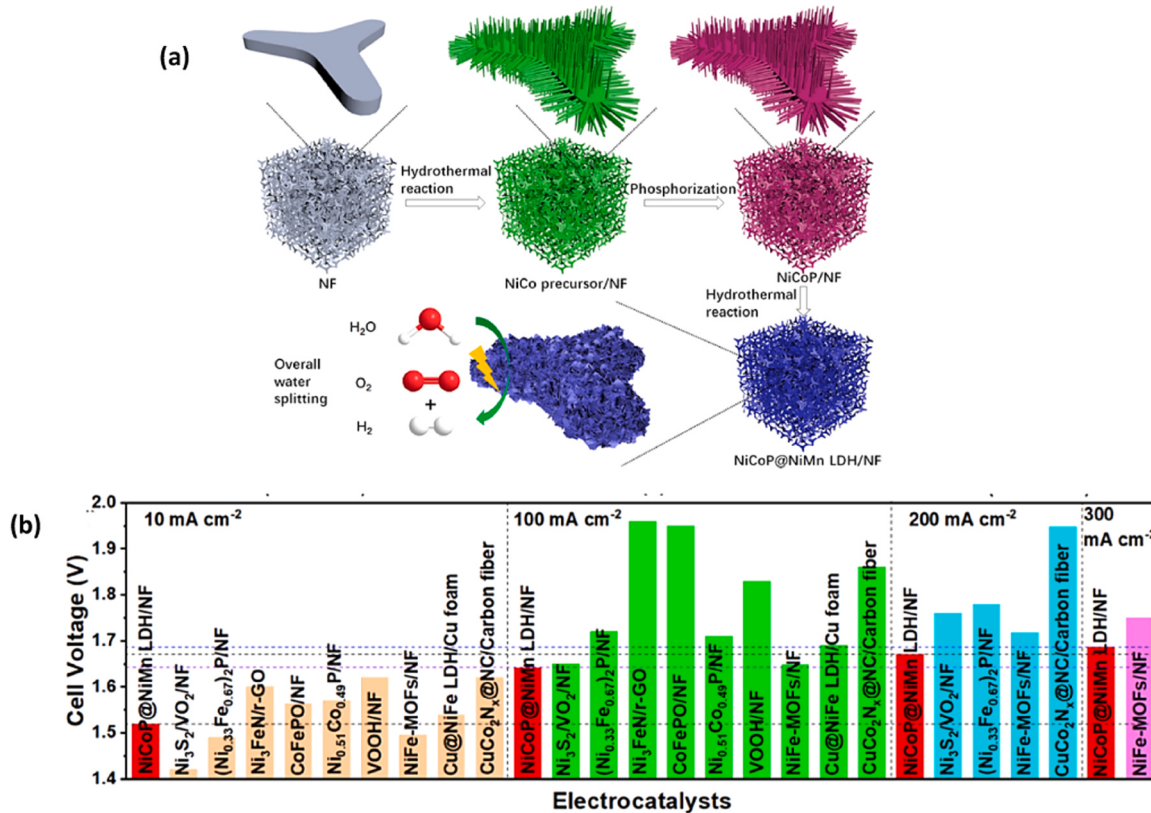


Fig. 15. (a) Schematic illustration of the fabricated process for the NiCoP@NiMn LDH/NF and (b) Comparison of cell voltages of different electrodes at 10, 100, 200, and 300 mA cm^{-2} for water-splitting. Reprinted with permission from [142]. Copyright (2020), American Chemical Society.

environmentally unsustainable and economically unfeasible. Metal chalcogenides (MCs), represented by the chemical formula MX_2 where 'M' stands for transition metal and 'X' represents a chalcogen, have emerged as promising alternatives to PGM-based electrocatalysts. They have garnered significant attention due to their diverse range of chemical, mechanical, optical, electronic, and thermal properties. Additionally, they are abundant, exhibit good conductivity, and, importantly, are more eco-friendly and economically viable [144–146]. Notably, MCs-based semiconductor photoelectrocatalysts have gained traction as potential candidates for environmental pollution degradation and hydrogen energy generation through the photoelectrolysis of water [147]. Over recent decades, various semiconductor-based photocatalysts, including nitrides and sulfides, have been developed to enhance their photocatalytic activities under UV-visible light irradiation [148,149].

For example, Chia and coworkers prepared three distinct electrocatalysts such as PtS_2 , PtSe_2 , and PtTe_2 , which exhibited promising HER performance with favorable overpotentials of 83, 63, and 54 mV@10 mA cm $^{-2}$, respectively [150]. Their Tafel slopes were measured at 216, 132, and 110 mV/dec, respectively. Density functional theory (DFT) study was conducted to explore the electronic and electrochemical behaviors of Pt dichalcogenides. From the DFT calculation, it was found that PtS_2 , PtSe_2 , and PtTe_2 have semiconductor, semi-metallic and metallic behavior. Moreover, among the Pt dichalcogenides, PtS_2 shows an exceptional catalytic response towards HER, which is estimated to be about 50% less over potential than other materials.

Moreover, a nano heterostructure composed of molybdenum selenide-supported tin sulfide nanosheets (MoSe_2/SnS) was synthesized using an in-situ technique [151]. The resulting MoSe_2/SnS electrocatalyst displayed increased active sites and improved rate transfer processes, particularly in applications related to water-splitting. The photoelectrode, comprising gold nanoparticle-supported zinc oxide-based cadmium sulfide nanotube arrays (Au NPs/ZnO/CdS NTAs), was effectively modified through electrochemical deposition and the chemical bath method, followed by an Au photoreduction process. The optimized photoelectrode exhibited exceptional photoelectrochemical performance under visible light conditions, showcasing a reported photocurrent density of 21.53 mA/cm 2 at 1.2 V and achieving a photoconversion efficiency (PCE) of 3.45% (Fig. 16) [152]. Moreover, Park *et al.* synthesized two distinct nanocrystal materials based on CoSe_2 and NiSe_2 bifunctional catalysts for the in-situ production of O_2 and H_2 via the water electrolysis process [153]. Among these electrocatalysts, NiSe_2 stands out as a promising candidate for use in water-splitting solar cell applications due to its oxide layer, which enhances its electrocatalytic activity.

3. Conclusions and future perspective

In this review, we have highlighted emerging strategies in the development of high-performance, 2D-based electrode materials for the process of (photo)electrochemical water splitting applications. Although

we have discussed the latest advancements, challenges and possible use in the field of (photo)electrochemical water-splitting, this study includes an overview of the essential functions and various manufacturing techniques of 2D-based composite photoelectrode materials. Green hydrogen fuel is among the most promising options capable of meeting future global energy demands. Developing affordable 2D electrode materials using various strategies capable of adjusting their energy levels is vital for producing hydrogen fuel via water (photo)electrolysis. These materials should possess an adaptable band gap and be economically viable for the photochemical process of splitting water into hydrogen and oxygen, generating energy.

In particular, some 2D-based electrode materials exhibit disadvantages such as low-rate performance, poor electrical conductivity, and limited cyclic durability, which hinder their potential for widespread use in large-scale electrochemical applications. For instance, numerous researchers have concentrated on developing 2D-based heterostructured materials to optimize their hierarchical structures, aiming to enhance their electrochemical performance and need to rectify these kinds of technological issues. In discussions about 2D-based photoelectrocatalysts, we aim to enhance their ability to transfer charges and improve their electrochemical properties. Another draw back of 2D materials is to obtain consistent, reproducible results due to the difficulty of controlling or growing a large surface area of materials with defect-free uniform thickness. In order to construct 2D materials with better integration of existing materials, novel fabrication approaches are necessary. The catalytic performance of the 2D materials was enhanced when they were incorporated with other conducting materials to form hybrid materials. Additionally, it is necessary to investigate the variation between monolayers and multilayers of 2D materials, the heterojunction characteristics as well as the effect of hybridization and surface modification in greater detail.

Further, as noted, ultrathin 2D materials significantly lose their intrinsic properties over the period of time. Thus, new techniques must be developed to store 2D materials for a longer period of time without causing the materials to lose their intrinsic properties. Moreover, 2D materials are found to encounter brittle/ductile failure thereby, it is important to investigate the materials in terms of mechanical strength related to material defects. Theoretical models like DFT calculations are a more effective way to study the electronic and electrochemical behaviors of materials. There are also opportunities in this field due to recent technological advancements that involve the use of Artificial Intelligence (AI) based predictive models.

Overall, this review will provide valuable insights for developing better 2D electrocatalysts with different structures. These improved materials can be more efficient in producing hydrogen through photocatalysis. The vast potential of 2D materials is still being investigated by researchers, so it is likely that 2D materials-based electrocatalysts for water splitting will soon be used for practical applications even though they have not been commercialized yet.

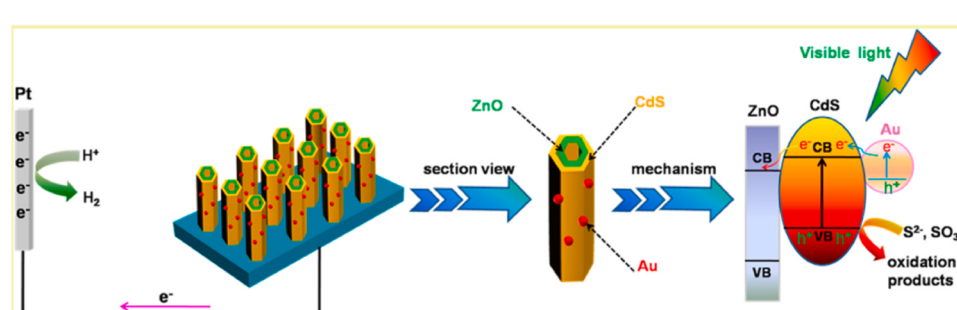


Fig. 16. Fabrication of $\text{ZnO}/\text{CdS}/\text{Au}$ NTAs photoanode and proposed charge carriers transfer mechanism in $\text{ZnO}/\text{CdS}/\text{Au}$ NTAs photoanode. Reprinted with permission from [152]. Copyright (2017), American Chemical Society.

CRediT author contributions statement

Conceptualization, T.-W.C., S.-M.C., P.K., G.A., R.K., A.G.A., V.M., S. A., M.M.A., S.J., T.C.M and R.R; Resources, T.-W.C., R.R., P.K., S.-M.C., G.A., A.G.A., and R.K; Supervision, S.-M.C., R.R., A.G.A., V.M., S.A., M.M.A., T.C.M and S.A. Writing-original draft preparation, T.-W.C., S.-M.C., R.R., P.K., G.A., A.G.A., V.M., M.M.A., T.C.M, S.J and R.R; Writing-review and editing, T.W.C., R.R., P.K and S.-M.C. All authors have read and agreed to the published version of the manuscript.

Institutional Review Board Statement

Not applicable.

Informed Consent Statement

Not applicable.

Funding

Please add: The financial support (NSTC 112-2113-M-027-001 to SMC) from the National Science and Technology Council (NSTC), Taiwan is appreciated. A.G.A. acknowledges support and funding of Deanship of Scientific Research, King Khalid University, Saudi Ara bia for Large Research Group under the grant number R.G.P. 2/121/1445.

Declaration of Competing Interest

The authors declare no conflict of interest.

Data Availability

Not applicable.

Appendix A. Supporting information

Supplementary data associated with this article can be found in the online version at [doi:10.1016/j.ijoe.2024.100576](https://doi.org/10.1016/j.ijoe.2024.100576).

References

- [1] J. Dar, M. Asif, Environmental feasibility of a gradual shift from fossil fuels to renewable energy in India: evidence from multiple structural breaks cointegration, *Renew. Energy* 202 (2023) 589–601, <https://doi.org/10.1016/j.renene.2022.10.131>.
- [2] U.K. Pata, S. Erdogan, O. Ozkan, Is reducing fossil fuel intensity important for environmental management and ensuring ecological efficiency in China? (<https://doi.org/10.1016/j.jenvman.2022.117080>, <https://doi.org/10.1016/j.jenvman.2022.117080>).
- [3] G.K. Karayel, I. Dincer, Green hydrogen production potential of Canada with solar energy, *Renew. Energy* (2023) 119766, <https://doi.org/10.1016/j.renene.2023.119766>.
- [4] Z. Zuo, M. Saraswat, I. Mahariq, T.U.K. Nutakki, A. Albani, A.H. Seikh, V.F. Lee, Multi-criteria thermoeconomic optimization of a geothermal energy-driven green hydrogen production plant coupled to an alkaline electrolyzer, *Process Saf. Environ. Prot.* 182 (2024) 154–165, <https://doi.org/10.1016/j.psep.2023.11.031>.
- [5] A. Smoliński, N. Howaniec, R. Gąsior, J. Polański, M. Magdziarczyk, Hydrogen rich gas production through co-gasification of low rank coal, flotation concentrates and municipal refuse derived fuel, *Energy* 235 (2021) 121348, <https://doi.org/10.1016/j.energy.2021.121348>.
- [6] M.A. Habib, M.A. Haque, A. Harale, S. Paglieri, F.S. Alrashed, A.A. Sayoud, M. A. Nemitallah, S. Hossain, A. Abuelyamen, E.M.A. Mokheimer, R.B. Mansour, Palladium-alloy membrane reactors for fuel reforming and hydrogen production: Hydrogen Production Modeling, *Case Stud. Therm. Eng.* 49 (2023) 103359, <https://doi.org/10.1016/j.csite.2023.103359>.
- [7] H. Yu, J. Wan, M. Goodsite, H. Jin, Advancing direct seawater electrocatalysis for green and affordable hydrogen, *One Earth* 6 (2023) 267–277, <https://doi.org/10.1016/j.oneear.2023.02.003>.
- [8] A.E. Karaca, I. Dincer, Development of a new photoelectrochemical system for clean hydrogen production and a comparative environmental impact assessment with other production methods, *Chemosphere* 337 (2023) 139367, <https://doi.org/10.1016/j.chemosphere.2023.139367>.
- [9] T.W. Chen, P. Kalimuthu, P. Veerakumar, S.M. Chen, G. Anushya, T. Jayapragasam, K.C. Lin, V. Mariyappan, R. Ramachandran, Review—Recent Advances in the Development of Porous Carbon-Based Electrocatalysts for Water-Splitting Reaction, *J. Electrochem. Soc.* 169 (2022) 054519, <https://doi.org/10.1149/1945-7111/ac6e91>.
- [10] T.W. Chen, G. Anushya, S.M. Chen, P. Kalimuthu, V. Mariyappan, P. Gajendran, R. Ramachandran, Recent advances in nanoscale based electrocatalysts for metal-air battery, fuel cell and water-splitting applications: an overview, *Materials* 15 (2) (2022) 458, <https://doi.org/10.3390/ma15020458>.
- [11] T.W. Chen, P. Kalimuthu, P. Veerakumar, K.C. Lin, S.M. Chen, R. Ramachandran, V. Mariyappan, S. Chitra, Recent Developments in Carbon-Based Nanocomposites for Fuel Cell Applications: A Review, *Molecules* 27 (3) (2022) 761, <https://doi.org/10.3390/molecules27030761>.
- [12] T.W. Chen, S.M. Chen, G. Anushya, R. Kannan, P. Veerakumar, M.M. Alam, S. Alargarsamy, R. Ramachandran, Metal-oxides- and metal-oxyhydroxides-based nanocomposites for water splitting: an overview, *Nanomaterials* 13 (13) (2023) 2012, <https://doi.org/10.3390/nano13132012>.
- [13] V.H. Nguyen, T.P. Nguyen, T.H. Le, D.V.N. Vo, D.L.T. Nguyen, Q.T. Trinh, I. T. Kim, Q.V. Le, Recent advances in two-dimensional transition metal dichalcogenides as photoelectrocatalyst for hydrogen evolution reaction, *J. Chem. Technol. Biotechnol.* 95 (10) (2020) 2597–2607, <https://doi.org/10.1002/jctb.6335>.
- [14] M.M. Ayyub, R. Singh, C.N.R. Rao, Hydrogen Generation by Solar Water Splitting Using 2D Nanomaterials, *Sol., RRL* 4 (8) (2020) 2000050, <https://doi.org/10.1002/solr.202000050>.
- [15] Y. Yang, S. Niu, D. Han, T. Liu, G. Wang, Y. Li, Progress in developing metal oxide nanomaterials for photoelectrochemical water splitting, *Adv. Energy Mater.* 7 (7) (2017) 1700555, <https://doi.org/10.1002/aenm.201700555>.
- [16] Z. Wang, X. Ma, Q. Li, X. Tian, J. Si, M.A. Melo, Fabrication of TiO₂ nanorods/γ-graphyne boosting junction-driven charge transfer for efficient photoelectrochemical water splitting, *Vacuum* 220 (2024) 112872, <https://doi.org/10.1016/j.vacuum.2023.112872>.
- [17] J. Wu, J. Wei, B. Lv, M. Wang, X. Wang, W. Wang, Enhanced solar-light-driven photoelectrochemical water splitting performance of type II 1D/OD CdS/In₂S₃ nanorod arrays, *Chem. Phys. Lett.* 830 (2023) 140776, <https://doi.org/10.1016/j.cplett.2023.140776>.
- [18] D. Liu, W. Jin, L. Zhang, Q. Li, Q. Sun, Y. Wang, X. Hu, H. Miao, Constructing 1D/OD Sb₂S₃/Cd_{0.6}Zn_{0.4}S-scheme heterojunction by vapor transport deposition and in-situ hydrothermal strategy towards photoelectrochemical water splitting, *J. Alloy. Compd.*, 975 (2024) 172926, <https://doi.org/10.1016/j.jallcom.2023.172926>.
- [19] M. Meng, L. Yang, J. Yang, Y. Zhu, C. Li, H. Xia, H. Yuan, M. Zhang, Y. Zhao, F. Tian, J. Li, K. Liu, L. Wang, Z. Gan, Two-dimensional lateral anatase-rutile TiO₂ phase junctions with oxygen vacancies for robust photoelectrochemical water splitting, *J. Colloid Interface Sci.* 648 (15) (2023) 56–65.
- [20] M.P. Niharika, R. Garlapally, K. Ruthvik, M. Velaga, B.M. Rao, Hydrogen production on g-C₃N₄ nanoflakes via photoelectrochemical water splitting, DOI: 10.1016/j.matpr.2023.06.188, *Mater. Today.: Proc.* (2023), <https://doi.org/10.1016/j.matpr.2023.06.188>.
- [21] L. Wang, W. Si, Y. Tong, F. Hou, D. Pergolesi, J. Hou, T. Lippert, S.X. Dou, J. Liang, Graphitic carbon nitride (g-C₃N₄)-based nanosized heteroarrays: Promising materials for photoelectrochemical water splitting, *Carbon Energy* 2 (2020) 223–225, <https://doi.org/10.1002/cey.248>.
- [22] R. Koutavarapu, T.G. S.G.Peera, C.R. Lee, D.Y. Myla, J. Lee, S.K. Shim, Balasingam, Recent Trends in Graphitic Carbon Nitride-Based Binary and Ternary Heterostructured Electrodes for Photoelectrochemical Water Splitting, *Processes* 9 (11) (2021) 1959, <https://doi.org/10.3390/pr9111959>.
- [23] W. Chen, T. Wang, J. Xue, S. Li, Z. Wang, S. Sun, Cobalt–nickel layered double hydroxides modified on tio2 nanoparticle arrays for highly efficient and stable pec water splitting, *Small* 13 (2017) 1602420, <https://doi.org/10.1002/smll.201602420>.
- [24] J. Yu, F. Yu, M.F. Yuenc, C. Wang, Two-dimensional layered double hydroxides as a platform for electrocatalytic oxygen evolution, *J. Mater. Chem. A* 9 (2021) 9389–9430, <https://doi.org/10.1039/DOTA11910E>.
- [25] T. Hong, Z. Liu, J. Zhang, G. Li, J. Liu, X. Zhang, S. Lin, Flower-like Cu₂In₂ZnS₅ Nanosheets: A Novel Promising Photoelectrode for Water Splitting, *Chem. Cat. Chem.* 8 (2016) 1288–1292, <https://doi.org/10.1002/cctc.201600066>.
- [26] L. Wang, Y. Li, Y. Liu, Reduced graphene oxide@TiO₂ nanorod@reduced graphene oxide hybrid nanostructures for photoelectrochemical hydrogen production, *Micro Nano Lett.* 12 (2017) 494–496, <https://doi.org/10.1049/mnl.2016.0747>.
- [27] Z. Luo, D. Zhang, C. Ma, M. Zhu, B. Li, L. Song, S. Yang, Nanoarchitecture of a Two-Dimensional Few-Layer Graphene Oxide/π-Conjugated Polyimide Composite for Enhanced Photocatalytic Performance, *ACS Omega* 8 (4) (2023) 4072–4080, <https://doi.org/10.1021/acsomega.2c07010>.
- [28] G. Zhuang, J. Yan, Y. Wen, Z. Zhuang, Y. Yu, Two-Dimensional Transition Metal Oxides and Chalcogenides for Advanced Photocatalysis: Progress, Challenges, and Opportunities, *RRL Sol.* 5 (2021) 2000403, <https://doi.org/10.1002/solr.202000403>.
- [29] A. Mondal, A. Vomiero, 2D Transition Metal Dichalcogenides-Based Electrocatalysts for Hydrogen Evolution Reaction, *Adv. Funct. Mater.* 32 (52) (2022) 2208994, <https://doi.org/10.1002/adfm.202208994>.
- [30] Y. Song, X. Zhang, Y. Zhang, P. Zhai, Z. Li, D. Jin, J. Cao, C. Wang, C. Zhang, B. Gao, J. Sun, L. Hou, Engineering Mo₃/MXene hole transfer layers for unexpected boosting of photoelectrochemical water oxidation, *J. Angew. Chem. Int. Ed.* 61 (2022) e202200946, <https://doi.org/10.1002/anie.202200946>.

- [31] Q. Lin, Y. Liu, Z. Yang, Z. He, H. Wang, L. Zhang, M.B.M.Y. Ang, G. Zeng, Construction and application of two-dimensional MXene-based membranes for water treatment: A mini-review, *Results Eng.* 15 (2022) 100494, <https://doi.org/10.1016/j.rineng.2022.100494>.
- [32] R. Tang, S. Zhou, C. Li, R. Chen, L. Zhang, Z. Zhang, L. Yin, Janus-Structured Co-Ti₃C₂ MXene Quantum Dots as a Schottky Catalyst for High-Performance Photoelectrochemical Water Oxidation, *Adv. Funct. Mater.* (2020) 2000637, <https://doi.org/10.1002/adfm.202000637>.
- [33] M. Ashraf, R. Ali, L. Khan, N. Ullah, M.S. Ahmad, T. Kida, S. Wooh, W. Tremel, U. Schwingenschlögl, M.N. Tahir, Bandgap engineering of melon using highly reduced graphene oxide for enhanced photoelectrochemical hydrogen evolution, *Adv. Mater.* 35 (2023) 2301342, <https://doi.org/10.1002/adma.202301342>.
- [34] C. Chen, Y. Lu, R. Fan, M. Shen, Integration of Oxygen-Vacancy-Rich NiFe-Layered Double Hydroxide onto Silicon as Photoanodes for Enhanced Photoelectrochemical Water Oxidation, *Chem. Sus. Chem.* 13 (2020) 3893–3900, <https://doi.org/10.1002/cssc.202000884>.
- [35] A. Loudiki, M. Azriouil, M. Matrouf, F. Laghrab, A. Farahi, S. Saqrane, M. Bakasse, S. Lahrich, M.A.F. Mhammedi, Graphene-based electrode materials used for some pesticide's detection in food samples: A review, *Inorg. Chem. Commun.* 14 (14) (2022) 109891, <https://doi.org/10.1016/j.inoche.2022.109891>.
- [36] Q. Ke, J. Wang, Graphene-based materials for supercapacitor electrodes-A review, *J. Mater.* 2 (1) (2016) 37–54, <https://doi.org/10.1016/j.jmat.2016.01.001>.
- [37] C. Xu, B. Xu, Y. Gu, Z. Xiong, J. Sun, X.S. Zhao, Graphene-based electrodes for electrochemical energy storage, *Energy Environ. Sci.* 6 (2013) 1388–1414, <https://doi.org/10.1039/C3EE23870A>.
- [38] A. Ambrosi, C.K. Chua, A. Bonanni, M. Pumera, Electrochemistry of Graphene and Related Materials, *Chem. Rev.* 114 (14) (2014) 7150–7188, <https://doi.org/10.1021/cr500023c>.
- [39] H. Omar, N.S.A. Malek, M.Z. Nurfazianawati, N.F. Rosman, I. Bunyamin, S. Abdullah, Z. Khusaimi, M. Rusop, N.A. Asli, A review of synthesis graphene oxide from natural carbon based coconut waste by Hummer's method, *Mater. Today.: Proc.* 75 (2023) 188–192, <https://doi.org/10.1016/j.mpr.2022.11.427>.
- [40] S. Khanna, P. Marathey, A. Vanpariya, S. Paneliya, I. Mukhopadhyay, In-situ preparation of titania/graphene nanocomposite via a facile sol-gel strategy: A promising anodic material for Li-ion batteries, *Mater. Lett.* 300 (2021) 130143, <https://doi.org/10.1016/j.matlet.2021.130143>.
- [41] E. Park, J. Ha, J. Lee, Y.T. Kim, J. Choi, Electrochemically exfoliated reduced graphene oxide-based freestanding separator-integrated electrode with embedded C-coated SiO_x as the current collector-free anode in flexible batteries, *J. Ind. Eng. Chem.* 131 (2024) 221–229, <https://doi.org/10.1016/j.jiec.2023.10.021>.
- [42] R. Siddiqui, M. Rani, A.A. Shah, A. Razzaq, R. Iqbal, R. Neffati, M. Arshad, Fabrication of tricarboxylate-neodymium metal organic frameworks and its nanocomposite with graphene oxide by hydrothermal synthesis for a symmetric supercapacitor electrode material, *Mater. Sci. Eng. B* 295 (2023) 116530, <https://doi.org/10.1016/j.mseb.2023.116530>.
- [43] Y. Zheng, S. Mao, J. Zhu, L. Fu, M. Moghadam, A scientometric study on application of electrochemical sensors for detection of pesticide using graphene-based electrode modifiers, *Chemosphere* 307 (2022) 136069, <https://doi.org/10.1016/j.chemosphere.2022.136069>.
- [44] H. Li, X. Wang, C. Li, X. Wang, X. Liu, B. Li, Y. Wu, First-principles study of quantum capacitance of transition metal oxides and nitrogen functionalized graphene as electrode materials for supercapacitor, *Phys. B Condens. Matter* 667 (2023) 415195, <https://doi.org/10.1016/j.physb.2023.415195>.
- [45] H. Qin, Z. Mo, J. Lu, X. Sui, Z. Song, B. Chen, Y. Zhang, Z. Zhang, X. Lei, A. Lu, Z. Mo, Ultrafast transformation of natural graphite into self-supporting graphene as superior anode materials for lithium-ion batteries, *Carbon* 216 (216) (2024) 118559, <https://doi.org/10.1016/j.carbon.2023.118559>.
- [46] K. Kaur, M. Patyal, N. Gupta, A. Kumar, M. Khanuani, Graphene/macrocyclic Yb nanocomposite as counter electrode in dye sensitized solar cell, *Opt. Mater.* 139 (2023) 113831, <https://doi.org/10.1016/j.optmat.2023.113831>.
- [47] G. Yang, J. Liu, M. Zhou, J. Bai, X. Bo, Fast and Facile Room-Temperature Synthesis of MOF-Derived Co Nanoparticle/Nitrogen-Doped Porous Graphene in Air Atmosphere for Overall Water Splitting, *ACS Sustain. Chem. Eng.* 8 (2020) 11947–11955, <https://doi.org/10.1021/acssuschemeng.0c01008>.
- [48] B. Sarkar, B.K. Barman, K.K. Nanda, Non-Precious Bimetallic Co-Cr Nanostructures Entrapped in Bamboo-like Nitrogen-doped Graphene Tube as a Robust Bi-functional Electrocatalyst for Total Water Splitting, *ACS Appl. Energy Mater.* 1 (3) (2018) 1116–1126, <https://doi.org/10.1021/acsaem.7b00233>.
- [49] J. Cirone, S.R. Ahmed, P.C. Wood, A. Chen, Green Synthesis and Electrochemical Study of Cobalt/Graphene Quantum Dots for Efficient Water Splitting, *J. Phys. Chem. C* 123 (2019) 9183–9191, <https://doi.org/10.1021/acs.jpcc.9b00951>.
- [50] R. Paul, M. Wang, A. Roy, Transparent Graphene/BN-Graphene Stacked Nanofilms for Electrocatalytic Oxygen Evolution, *ACS Appl. Nano Mater.* (2020) 10418–10426, <https://doi.org/10.1021/acsnano.0c02307>.
- [51] W. Ma, R. Ma, C. Wang, J. Liang, X. Liu, K. Zhou, T. Sasaki, A. Superlattice, of Alternately Stacked Ni-Fe Hydroxide Nanosheets and Graphene for Efficient Splitting of Water, *ACS Nano* 9 (2) (2015) 1977–1984, <https://doi.org/10.1021/nm5069836>.
- [52] L. Li, X. Wang, Y. Guo, J. Li, Synthesis of an Ultrafine CoP Nanocrystal/Graphene Sandwiched Structure for Efficient Overall Water Splitting, *Langmuir* 36 (8) (2020) 1916–1922, <https://doi.org/10.1021/acs.langmuir.9b03810>.
- [53] Saima Noreen, H.N. Bhatti, M. Iqbal, F. Hussain, F.M. Sarim, Chitosan, starch, polyaniline and polypyrrrole biocomposite with sugarcane bagasse for the efficient removal of Acid Black dye, *Int. J. Biol. Macromol.* 147 (2020) 439–452, <https://doi.org/10.1016/j.ijbiomac.2019.12.257>.
- [54] B.C. Hodges, E.L. Cates, J.H. Kim, Challenges and prospects of advanced oxidation water treatment processes using catalytic nanomaterials, *Nat. Nanotechnol.* 13 (8) (2018) 642–650, <https://doi.org/10.1038/s41565-018-0216-x>.
- [55] L. Ma, et al., Fabrication and water treatment application of carbon nanotubes (CNTs)-based composite membranes: a review, *Membranes* 7 (1) (2017) 16, <https://doi.org/10.3390/membranes7010016>.
- [56] L. Chi, Y. Qian, J. Guo, X. Wang, H. Arandiyani, Z. Jiang, Novel g-C₃N₄/TiO₂/PAA/PTFE ultrafiltration membrane enabling enhanced antifouling and exceptional visible-light photocatalytic self-cleaning, *Catal. Today* 335 (2019) 527–537, <https://doi.org/10.1016/j.cattod.2019.02.027>.
- [57] X. Li, G. Huang, X. Chen, J. Huang, M. Li, J. Yin, Y. Liang, Y. Yao, Y. Li, A review on graphitic carbon nitride (g-C₃N₄) based hybrid membranes for water and wastewater treatment, *Sci. Total Environ.* 792 (2021) 148462, <https://doi.org/10.1016/j.scitotenv.2021.148462>.
- [58] Z. Chen, S. Zhang, Y. Liu, N.S. Alharbi, S.O. Rabah, S. Wang, X. Wang, Synthesis and fabrication of g-C₃N₄-based materials and their application in the elimination of pollutants, *Sci. Total Environ.* 731 (2020) 139054, <https://doi.org/10.1016/j.scitotenv.2020.139054>.
- [59] B. Zhang, J. Li, "Electron Complementation"-Induced Molybdenum Nitride/Co Anchored Graphitic Carbon Nitride Porous Nanoparticles for Efficient Overall Water Splitting, *Inorg. Chem.* 61 (49) (2022) 20095–20104, <https://doi.org/10.1021/acs.inorgchem.2c03516>.
- [60] S.B. Sundararaj, S. Tamilarasan, S. Thangavelu, Layered Porous Graphitic Carbon Nitride Stabilized Effective Co₂SnO₄ Inverse Spinel as a Bifunctional Electrocatalyst for Overall Water Splitting, *Langmuir* 38 (25) (2022) 7833–7845, <https://doi.org/10.1021/acs.langmuir.2c01095>.
- [61] Z. Chen, Y. Ha, Y. Liu, H. Wang, H. Yang, H. Xu, Y. Li, R. Wu, In Situ Formation of Cobalt Nitrides/Graphitic Carbon Composites as Efficient Bifunctional Electrocatalysts for Overall Water Splitting, *ACS Appl. Mater. Interfaces* 10 (2018) 7134–7144, <https://doi.org/10.1021/acsami.7b18858>.
- [62] B. Wang, F. Shi, Y. Sun, L. Yan, X. Zhang, B. Wang, W. Sun, Ni-enhanced molybdenum carbide loaded N-doped graphitized carbon as bifunctional electrocatalyst for overall water splitting, *Appl. Surf. Sci.* 572 (2022) 151480, <https://doi.org/10.1016/j.apsusc.2021.151480>.
- [63] T. Bhowmik, M.K. Kundu, S. Barman, CoFe Layered Double Hydroxide Supported on Graphitic Carbon Nitrides: An Efficient and Durable Bi-functional Electrocatalyst for Oxygen Evolution and Hydrogen Evolution Reactions, *ACS Appl. Energy Mater.* 1 (3) (2018) 1200–1209, <https://doi.org/10.1021/acsaem.7b00305>.
- [64] S. Zhao, Y. Liu, Y. Wang, L. Xie, J. Fang, Y. Zhang, Y. Zhou, S. Zhuo, C-Rich Graphitic Carbon Nitride with Cross-Pore Channels: A Visible Light-Driven Photocatalyst for Water Splitting, *ACS Appl. Energy Mater.* 4 (2021) 1784–1792, <https://doi.org/10.1021/acsaelm.0c02924>.
- [65] B. Xu, S. Li, Q. Zhao, S. Feng, X. Peng, P.K. Chu, Electrochemical reduction of nitrate to ammonia using non-precious metal-based catalysts, *Coord. Chem. Rev.* 502 (2024) 215609, <https://doi.org/10.1016/j.ccr.2023.215609>.
- [66] R. Huang, J. Wang, S. Liu, Y. Yang, W. Deng, Y. Su, Non-precious transition metal based electrocatalysts for vanadium redox flow batteries: Rational design and perspectives, *J. Power Sources* 515 (2021) 230640, <https://doi.org/10.1016/j.jpowsour.2021.230640>.
- [67] K. Manojkumar, R. Kandeeban, R. Brindha, V. Sangeetha, K. Saminathan, Non-precious metal-based integrated electrodes for overall alkaline water splitting, *J. Indian Chem. Soc.* 99 (2022) 100775, <https://doi.org/10.1016/j.jics.2022.100775>.
- [68] J. Pan, C. Li, Y. Peng, L. Wang, B. Li, G. Zheng, M. Song, Application of transition metal (Ni, Co and Zn) oxides-based electrode materials for ion-batteries and supercapacitors, *Int. J. Electrochem. Sci.* 18 (2023) 100233, <https://doi.org/10.1016/j.ijoe.2023.100233>.
- [69] R. Wang, N. Wang, X. Zhang, M. Xie, L. Huang, Q. Zhang, C. Feng, Y. Xu, Y. Jiao, J. Chen, Inhibiting solubility challenges: Carbon nanotube encapsulation of stable transition metal oxides for electrochemical energy storage and conversion applications, *J. Energy Storage* 76 (2024) 109794, <https://doi.org/10.1016/j.est.2023.109794>.
- [70] J. Ganeshamurthy, R. Shanmugam, S.M. Chen, K. Alagumalai, M. Balamurugan, C., H. Fan, A portable electrochemical sensor based on binary transition metal oxide (CoO/ZnO) for the evaluation of eugenol in real-time samples, *Surf. Interfaces* 38 (2023) 102845, <https://doi.org/10.1016/j.surfin.2023.102845>.
- [71] H. Li, X. Wang, C. Li, X. Wang, X. Liu, B. Li, Y. Wu, First-principles study of quantum capacitance of transition metal oxides and nitrogen functionalized graphene as electrode materials for supercapacitor, *Phys. B: Condens. Matter* 667 (2023) 415195, <https://doi.org/10.1016/j.physb.2023.415195>.
- [72] P. Pattanayak, P. Singh, N.K. Bansal, M. Paul, H. Dixit, S. Porwal, S. Mishra, T. Singh, Recent progress in perovskite transition metal oxide-based photocatalyst and photoelectrode materials for solar-driven water splitting, *J. Environ. Chem. Eng.* 10 (2022) 108429, <https://doi.org/10.1016/j.jece.2022.108429>.
- [73] Z. Shaghaghi, S. Jafari, R.M. Rezaei, The heterostructure of ceria and hybrid transition metal oxides with high electrocatalytic performance for water splitting and enzyme-free glucose detection, *J. Electroanal. Chem.* 915 (2022) 116369, <https://doi.org/10.1016/j.jelechem.2022.116369>.
- [74] G. He, Y. Liao, Y. Zhao, Y.E. Zhang, E. Yifeng, Construction of transition metal/metal oxide synergistic with carbon nanomaterials trinity composites to promote electrocatalytic oxygen evolution, *Int. J. Hydrog. Energy* 51 (2024) 231–241, <https://doi.org/10.1016/j.ijhydene.2023.09.308>.
- [75] X. Zhang, C.L. Dong, Y. Wang, J. Chen, K.T. Arul, Z. Diao, Y. Fu, M. Li, S. Shen, Regulating Crystal Structure and Atomic Arrangement in Single Component Metal

- Oxides through Electrochemical Conversion for Efficient Overall Water Splitting, *ACS Appl. Mater. Interfaces* 12 (51) (2020) 57038–57046, <https://doi.org/10.1021/acsami.0c16659>.
- [76] W. Chen, H. Wang, Y. Li, Y. Liu, J. Sun, S. Lee, J.S. Lee, Y. Cui, In Situ Electrochemical Oxidation Tuning of Transition Metal Disulfides to Oxides for Enhanced Water Oxidation, *ACS Cent. Sci.* 1 (5) (2015) 244–251, <https://doi.org/10.1021/acscentsci.5b00227>.
- [77] Y.H. Su, S.H. Huang, P.Y. Kung, T.W. Shen, W.L. Wang, Hydrogen Generation of Cu_2O Nanoparticles/ $\text{MnO}-\text{MnO}_2$ Nanorods Heterojunction Supported on Sonochemical-assisted Synthesized Few-Layer Graphene in Water Splitting Photocathode, *ACS Sustain. Chem. Eng.* 3 (9) (2015) 1965–1973, <https://doi.org/10.1021/acssuschemeng.5b00579>.
- [78] N. Li, X. Xu, B. Sun, K. Xie, W. Huang, T. Yu, Recent nanosheet-based materials for monovalent and multivalent ions storage, *Energy Stor. Mater.* 25 (2020) 382–403, <https://doi.org/10.1016/j.ensm.2019.10.002>.
- [79] N.D. Zaulkiflee, A.L. Ahmad, S.C. Low, N. Norikazu, Recent advances on the utilization of nanosheets as electrode material for supercapacitor application, *J. Energy Storage* 55 (2022) 105697, <https://doi.org/10.1016/j.est.2022.105697>.
- [80] S. Ali, X. Zhang, M.S. Javed, X. Zhang, G. Liu, X. Wei, H. Chen, M. Imran, J. Wang, W. Han, J. Qi, 2H-MoS₂ nanosheets-based binder-free electrode material for supercapacitor, *J. Appl. Phys.* 132 (2022) 145001, <https://doi.org/10.1063/5.0100522>.
- [81] M. Tawalbeh, H.A. Khan, A.A. Othman, Insights on the applications of metal oxide nanosheets in energy storage systems, *J. Energy Storage* 60 (2023) 106656, <https://doi.org/10.1016/j.est.2023.106656>.
- [82] I.H. Kwak, H.S. Im, D.M. Jang, Y.W. Kim, K. Park, Y.R. Lim, E.H. Cha, J. Park, CoSe₂ and NiSe₂ nanocrystals as superior bifunctional catalysts for electrochemical and photoelectrochemical water splitting, *ACS Appl. Mater. Interfaces* 8 (2016) 5327–5334, <https://doi.org/10.1021/acsami.5b12093>.
- [83] X. Wu, D. He, H. Zhang, H. Li, Z. Li, B. Yang, Z. Lin, L. Lei, X. Zhang, Ni_{0.85}Se as an efficient non noble bifunctional electrocatalyst for full water splitting, *Int. J. Hydrog. Energy* 41 (2016) 10688–10694, <https://doi.org/10.1016/j.ijhydene.2016.05.010>.
- [84] J. Zhou, Y. Liu, Z. Zhang, Z. Huang, X. Chen, X. Ren, L. Ren, X. Qi, J. Zhong, Hierarchical NiSe₂ sheet-like nano-architectures as an efficient and stable bifunctional electrocatalyst for overall water splitting: Phase and morphology engineering, *Electrochim. Acta* 279 (2018) 195–203, <https://doi.org/10.1016/j.electacta.2018.05.063>.
- [85] L. Hui, D. Jia, H. Yu, Y. Xue, Y. Li, Ultrathin Graphdiyne-Wrapped Iron Carbonate Hydroxide Nanosheets toward Efficient Water Splitting, *ACS Appl. Mater. Interfaces* 11 (3) (2019) 2618–2625, <https://doi.org/10.1021/acsami.8b01887>.
- [86] M. Zhai, F. Wang, H. Du, Transition-Metal Phosphide–Carbon Nanosheet Composites Derived from Two-Dimensional Metal-Organic Frameworks for Highly Efficient Electrocatalytic Water-Splitting, *ACS Appl. Mater. Interfaces* 9 (2017) 40171–40179, <https://doi.org/10.1021/acsami.7b10680>.
- [87] M. Rafiq, X. Hu, Z. Ye, A. Qayum, H. Xia, L. Hu, F. Lu, P.K. Chu, Recent advances in structural engineering of 2D hexagonal boron nitride electrocatalysts, *Nano Energy* 91 (2022) 106661, <https://doi.org/10.1016/j.nanoen.2021.106661>.
- [88] Y. Chen, J. Cai, P. Li, G. Zhao, G. Wang, Y. Jiang, J. Chen, S.X. Dou, H. Pan, W. Sun, Hexagonal Boron Nitride as a Multifunctional Support for Engineering Efficient Electrocatalysts toward the Oxygen Reduction Reaction, *Nano Lett.* 20 (9) (2020) 6807–6814, <https://doi.org/10.1021/acs.nanolett.0c02782>.
- [89] C. Sharma, P. Vanishree, B. Rani, N. Lohia, C. Swati, R. Srivastava, S.N. Sharma, Electrochemical properties of two-dimensional hexagonal boron nitride nanosheets prepared by hydrothermal method, *Electrochim. Acta* 463 (2023) 142848, <https://doi.org/10.1016/j.electacta.2023.142848>.
- [90] S. Angizi, M. Khalaj, S.A.A. Aleem, A. Pakdel, M. Willander, A. Hatamie, A. Simchi, Review-towards the two-dimensional hexagonal boron nitride (2D h-BN) electrochemical sensing platforms, *J. Electrochem. Soc.* 167 (2020) 167 126513, <https://doi.org/10.1149/1945-7111/abaf29>.
- [91] H. Garg, S. Patial, P. Raizada, V.H. Nguyen, S.Y. Kim, Q.V. Le, T. Ahamed, S. M. Alshehri, C.M. Hussain, T.T.H. Nguyen, P. Singh, Hexagonal-boroncarbonitrile (h-BCN) based heterostructure photocatalyst for energy and environmental applications: A review, *Chemosphere* 313 (2023) 137610, <https://doi.org/10.1016/j.chemosphere.2022.137610>.
- [92] S. Wang, J. Crowther, H. Kageshima, H. Hibino, Y. Taniyasu, Epitaxial Intercalation Growth of Scalable Hexagonal Boron Nitride/Graphene Bilayer Moiré Materials with Highly Convergent Interlayer Angles, *ACS Nano* 15 (9) (2021) 14384–14393, <https://doi.org/10.1021/acsnano.1c03698>.
- [93] Y. Chen, J. Cai, P. Li, G. Zhao, G. Wang, Y. Jiang, J. Chen, S.X. Dou, H. Pan, W. Sun, Hexagonal Boron Nitride as a Multifunctional Support for Engineering Efficient Electrocatalysts toward the Oxygen Reduction Reaction, *Nano Lett.* 20 (2020) 6807–6814, <https://doi.org/10.1021/acs.nanolett.0c02782>.
- [94] L. Song, S. Zhang, S. Sun, J. Wei, E. Liu, Performance and mechanism on hydrogen evolution of two-dimensional boron nitride under mechanical vibration, *Fuel* 331 (2023) 125765, <https://doi.org/10.1016/j.fuel.2022.125765>.
- [95] A.R. Aghjehkohal, A.T. Tabrizi, M. Yildiz, Electrochemical hydrogen storage of synthesized heterostructure of hexagonal boron nitride-carbon nano tube, *J. Alloy. Compd.* 962 (2023) 171159, <https://doi.org/10.1016/j.jallcom.2023.171159>.
- [96] N.E.F. Tapia, V. Valverde, G. Moreano, S. Chandra, L. Buenaño, A.I. Saber, H. Bahair, P. Singh, Y. Elmasry, The outstanding electrochemical performance of porous hexagonal boron nitride as a K-ion battery anode, *Inorg. Chem. Commun.* (2023) 111816, <https://doi.org/10.1016/j.inoche.2023.111816>.
- [97] B. Karuppaiah, A. Jeyaraman, S.M. Chen, Y.C. Huang, Development of highly sensitive electrochemical sensor for antibiotic drug ronidazole based on spinel cobalt oxide nanorods embedded with hexagonal boron nitride, *Electrochim. Acta* (2023) 142008, <https://doi.org/10.1016/j.electacta.2023.142008>.
- [98] Y. Lu, B. Li, N. Xu, Z. Zhou, Y. Xiao, Y. Jiang, T. Li, S. Hu, Y. Gong, Y. Cao, One-atom-thick hexagonal boron nitride co-catalyst for enhanced oxygen evolution reactions, *Nat. Commun.* 14 (2023) 6965, <https://doi.org/10.1038/s41467-023-42696-3>.
- [99] T.W. Chen, R. Ramachandran, S.M. Chen, N. Kavitha, K. Dinakaran, R. Kannan, G. Anushya, N. Bhuvana, T. Jayaprakasham, V. Mariyappan, S.D. Rani, S. Chitra, Developing Low-Cost, High Performance, Robust and Sustainable Perovskite Electrocatalytic Materials in the Electrochemical Sensors and Energy Sectors: "An Overview", *Catalysts* 10 (8) (2020) 938, <https://doi.org/10.3390/catal10080938>.
- [100] M. Mohan, N.P. Shetti, T.M. Aminabhavi, Perovskites: A new generation electrode materials for storage applications, *J. Power Sources* 574 (2023) 233166, <https://doi.org/10.1016/j.jpowsour.2023.233166>.
- [101] Y. Cao, J. Liang, X. Li, L. Yue, Q. Liu, S. Lu, A.M. Asiri, J. Hu, Y. Luo, X. Sun, Recent advances in perovskite oxides as electrode materials for supercapacitors, *Chem. Commun.* 57 (2021) 2343–2355, <https://doi.org/10.1039/DOCC07970G>.
- [102] H.S. Nan, X.Y. Hu, H.W. Tian, Recent advances in perovskite oxides for anion-intercalation supercapacitor: A review, *Mater. Sci. Semicond. Process.* 94 (2019) 35–50, <https://doi.org/10.1016/j.mssp.2019.01.033>.
- [103] B. Hua, M. Li, W. Pang, W. Tang, S. Zhao, Z. Jin, Y. Zeng, S. Amirkhiz, J.L. Luo, Activating p-blocking centres in perovskite for efficient water splitting, *Chem* 4 (12) (2018) 2902–2916, <https://doi.org/10.1016/j.chempr.2018.09.012>.
- [104] W. Wang, M. Xu, X. Xu, W. Zhou, Z. Shao, Perovskite oxide based electrodes for high-performance photoelectrochemical water splitting, *Angew. Chem., Int. Ed.* 59 (1) (2020) 136–152, <https://doi.org/10.1002/anie.201900292>.
- [105] J. Yu, X. Wu, D. Guan, Z. Hu, S.C. Weng, H. Sun, Y. Song, R. Ran, W. Zhou, M. Ni, Z. Shao, Monoclinic SrIrO₃: an easily-synthesized conductive perovskite oxide with outstanding performance for overall water splitting in alkaline solution, *Chem. Mater.* 32 (11) (2020) 4509–4517.
- [106] H. Park, I.J. Park, M.G. Lee, K.C. Kwon, S.P. Hong, D.H. Kim, S.A. Lee, T.H. Lee, C. Kim, C.W. Moon, D.Y. Son, G.H. Jung, H.S. Yang, J.R. Lee, J. Lee, N.G. Park, S. Y. Kim, J.Y. Kim, H.W. Jang, Water Splitting Exceeding 17% Solar-to-Hydrogen Conversion Efficiency Using Solution-Processed Ni-Based Electrocatalysts and Perovskite/Si Tandem Solar Cell, *ACS Appl. Mater. Interfaces* 11 (2019) 33835–33843, <https://doi.org/10.1021/acsami.9b09344>.
- [107] X. Sun, Y. Mi, F. Jiao, X. Xu, Activating layered perovskite compound Sr₂TiO₄ via La/N co-doping for visible light photocatalytic water splitting, *ACS Catal.* 8 (4) (2018) 3209–3221, <https://doi.org/10.1021/acs.catal.8b00369>.
- [108] L. Shi, W. Zhou, Z. Li, S. koul, A. Kushima, Y.A. Yang, Periodically Ordered Nanoporous perovskite photoelectrode for efficient photoelectrochemical water splitting, *ACS Nano* 12 (6) (2018) 6335–6342, <https://doi.org/10.1021/acsnano.8b03940>.
- [109] A.M. Idris, T. Liu, J.H. Shah, H. Han, C. Li, Sr₂CoTaO₆ Double Perovskite Oxide as a Novel visible-light-absorbing bifunctional photocatalyst for photocatalytic oxygen and hydrogen evolution reactions, *ACS Sustain. Chem. Eng.* 8 (2020) 14190–14197, <https://doi.org/10.1021/acssuschemeng.0c05237>.
- [110] M.A.H. Shontoa, M.I. Chowdhurya, A.B. Antub, N.R. Niloyc, N. Alama, M. A. Ullaha, M.S. Anowar, MXene based Heterostructures for electrode materials of Batteries: A Review, *IOP Conf. Ser.: Mater. Sci. Eng.* 1225 (2022) 012018, <https://doi.org/10.1088/1757-899X/1225/1/012018>.
- [111] H.J. Liu, B. Dong, Recent advances and prospects of MXene-based materials for electrocatalysis and energy storage, *Mater. Today Phys.* 20 (2021) 100469, <https://doi.org/10.1016/j.mtphys.2021.100469>.
- [112] I. Hussain, C. Lamiel, M.S. Javed, M. Ahmad, S. Sahoo, X. Chen, N. Qin, S. Iqbal, S. Gu, Y. Li, C. Chatzichristodoulou, K. Zhang, MXene-based heterostructures: current trend and development in electrochemical energy storage devices, *Prog. Energy Combust. Sci.* 97 (2023) 101097, <https://doi.org/10.1016/j.procs.2023.101097>.
- [113] D. Gandla, Z. Zhuang, V.V. Jadhav, D.Q. Tan, Lewis acid molten salt method for 2D MXene synthesis and energy storage applications: A review, *Energy Stor. Mater.* 63 (2023) 102977, <https://doi.org/10.1016/j.ensm.2023.102977>.
- [114] Y. Yu, Q. Fan, Z. Li, P. Fu, MXene-based electrode materials for supercapacitors: Synthesis, properties, and optimization strategies, *Mater. Today Sustain.* 24 (2023) 100551, <https://doi.org/10.1016/j.mtsust.2023.100551>.
- [115] Y. Li, S. Arnold, S. Husmann, V. Presser, Recycling and second life of MXene electrodes for lithium-ion batteries and sodium-ion batteries, *J. Energy Storage* 60 (2023) 106625, <https://doi.org/10.1016/j.est.2023.106625>.
- [116] L. Giebelner, J. Balach, MXenes in lithium-sulfur batteries: Scratching the surface of a complex 2D material - A minireview, *Mater. Today Commun.* 27 (2021) 102323, <https://doi.org/10.1016/j.mtcomm.2021.102323>.
- [117] M.B. Bahari, C.R. Mamat, A.A. Jalil, N.S. Hassan, N.F. Khusnun, M.H. Sawal, N. M. Izzudin, A.H. Hatta, S.H. Zein, V.G. Le, Advances in MXene-based photoanodes for water-splitting, *J. Electroanal. Chem.* 947 (2023) 117750, <https://doi.org/10.1016/j.jelechem.2023.117750>.
- [118] M. Li, S. Zhou, R. Sun, S. Han, J. Jiang, Hierarchical electronic coupling engineering of bimetallic sulfide driven by CoFe bimetal MOFs anchored on MXene promotes efficient overall water splitting, *Fuel* 358 (2024) 130256, <https://doi.org/10.1016/j.fuel.2023.130256>.
- [119] M.S.A. Zahra, M. Murshed, U. Naeem, T.M. Gesing, S. Rizwan, Cation-assisted self-assembled pillared V₂CTx MXene electrodes for efficient energy storage, *J. Chem. Eng.* 474 (2023) 145526, <https://doi.org/10.1016/j.cej.2023.145526>.

- [120] B. Shen, X. Liao, X. Zhang, H.T. Ren, J.H. Lin, C.W. Lou, T.T. Li, Synthesis of Nb₂C MXene-based 2D layered structure electrode material for high-performance battery-type supercapacitors, *Electrochim. Acta* 413 (2022) 140144, <https://doi.org/10.1016/j.electacta.2022.140144>.
- [121] S.G. Sarwar, I.L. Ikhioya, S. Afzal, I. Ahmad, Supercapitance performance evaluation of MXene/Graphene/NiO composite electrode via *in situ* precipitation technique, *Hybrid. Adv.* 4 (2023) 100105, <https://doi.org/10.1016/j.hybadv.2023.100105>.
- [122] X. Xie, R. Wang, Y. Ma, J. Chen, Q. Cui, Z. Shi, Z. Li, H. Xu, Photothermal-Effect-Enhanced Photoelectrochemical Water Splitting in MXene-Nanosheet-Modified ZnO Nanorod Arrays, *ACS Appl. Nano Mater.* 5 (8) (2022) 11150–11159, <https://doi.org/10.1021/acsanm.2c02302>.
- [123] P. Sharma, S. Kainth, O.P. Pandey, R. Mahajan, Customized Synthesis of 2D TiC MXene for Improved Overall Water Splitting, *ACS Appl. Nano Mater.* 6 (23) (2023) 21788–21802, <https://doi.org/10.1021/acsanm.3c03986>.
- [124] M. Li, R. Sun, Y. Li, J. Jiang, W. Xu, H. Cong, S. Han, The 3D porous “celosia” heterogeneous interface engineering of layered double hydroxide and P-doped molybdenum oxide on MXene promotes overall water-splitting, *J. Chem. Engin.* 431 (2022) 133941, <https://doi.org/10.1016/j.jce.2021.133941>.
- [125] A. Ravendran, M. Chandran, M.R. Siddiqui, S.M. Wabaidur, M. Eswaran, R. Dhanusuraman, Layer-by-Layer Assembly of CTAB-rGO-Modified MXene Hybrid Films as Multifunctional Electrodes for Hydrogen Evolution and Oxygen Evolution Reactions, Supercapacitors, and DMFC Applications, *ACS Omega* 8 (38) (2023) 34768–34786, <https://doi.org/10.1021/acsomega.3c03827>.
- [126] Q. Yue, J. Sun, S. Chen, Y. Zhou, H. Li, Y. Chen, R. Zhang, G. Wei, Y. Kang, Hierarchical mesoporous MXene-NiCoP electrocatalyst for water-splitting, *ACS Appl. Mater. Interfaces* 12 (16) (2020) 18570–18577, <https://doi.org/10.1021/acsmami.0c01303>.
- [127] D.N. Nguyen, G.S. Gund, M.G. Jung, S.H. Roh, J. Park, J.K. Kim, H.S. Park, Core-Shell Structured MXene@Carbon Nanodots as Bifunctional Catalysts for Solar-Assisted Water Splitting, *ACS Nano* 14 (12) (2020) 17615–17625, <https://doi.org/10.1021/acsnano.0c08436>.
- [128] M. Shao, R. Zhang, Z. Li, M. Wei, D.G. Evans, X. Duan, Layered double hydroxides toward electrochemical energy storage and conversion: design, synthesis and applications, *Chem. Commun.* 51 (15) (2015) 880–15893, <https://doi.org/10.1039/C5CC07296D>.
- [129] N. Baig, M. Sajid, Applications of layered double hydroxides based electrochemical sensors for determination of environmental pollutants: A review, *Trends Environ. Anal. Chem.* 16 (2017) 1–15, <https://doi.org/10.1016/j.teac.2017.10.003>.
- [130] R.C. Rohit, A.D. Jagadale, S.K. Shinde, D.Y. Kim, A review on electrodeposited layered double hydroxides for energy and environmental applications, *Mater. Today Commun.* 27 (2021) 102275, <https://doi.org/10.1016/j.mtcomm.2021.102275>.
- [131] S.N. Kanimozh, B. Aljafari, R. Singh, S. Anandan, M. Ashokkumar, Rod-like manganese-cobalt layered double hydroxides for the development of supercapacitor electrodes, *Nano-Struct. Nano-Objects* 36 (2023) 101044, <https://doi.org/10.1016/j.nano.2023.101044>.
- [132] J. Ma, L. Liu, T. He, J. Wu, J. Dai, Y. Dong, S. Lei, Y. Cai, Layered double hydroxide derived cobalt-iron sulfide heterostructures with enhanced reaction kinetics for use in sodium-ion batteries, *J. Alloy. Compd.* 927 (2022) 167088, <https://doi.org/10.1016/j.jallcom.2022.167088>.
- [133] S. Jia, Y. Liang, N. Yang, High performance of polyacrylonitrile/[MgAl]-layered double hydroxide composite nanofiber separators for safe lithium-ion batteries, *Solid State Ion.* 370 (2021) 115735, <https://doi.org/10.1016/j.ssi.2021.115735>.
- [134] S.H. Bendary, A.A. Abdelrahman, Flexible and novel counter electrode from graphene/Zn Al layered double hydroxide nanocomposite in dye sensitized solar cells, *J. Electroanal. Chem.* 922 (2022) 116736, <https://doi.org/10.1016/j.jelechem.2022.116736>.
- [135] P.R. Chowdhury, H. Medhi, K.G. Bhattacharyya, C.M. Hussain, Layered double hydroxides derived from waste for highly efficient electrocatalytic water splitting: Challenges and implications towards circular economy driven green energy, *Coord. Chem. Rev.* 501 (2024) 215547, <https://doi.org/10.1016/j.ccr.2023.215547>.
- [136] X. Zhang, A.N. Marianov, Y. Jiang, C. Cazorla, D. Chu, Hierarchically Constructed Silver Nanowire@Nickel-Iron Layered Double Hydroxide Nanostructures for Electrocatalytic Water Splitting, *ACS Appl. Nano Mater.* 3 (2020) 887–895, <https://doi.org/10.1021/acsanm.9b02457>.
- [137] S. Dutta, A. Indra, Y. Feng, T. Song, U. Paik, Self-Supported Nickel Iron Layered Double Hydroxide-Nickel Selenide Electrocatalyst for Superior Water Splitting Activity, *ACS Appl. Mater. Interfaces* 9 (2017) 33766–33774, <https://doi.org/10.1021/acsmami.7b07984>.
- [138] B. Chen, Z. Zhang, S. Kim, S. Lee, J. Lee, W. Kim, K. Yong, Ostwald Ripening Driven Exfoliation of Ultrathin Layered Double Hydroxides Nanosheets for Enhanced Oxygen Evolution Reaction (<https://doi.org/10.1021/acsmami.8b16962>).
- [139] G. Rajeshkhanna, T.I. Singh, N.H. Kim, J.H. Lee, Remarkable bi-functional oxygen and hydrogen evolution electrocatalytic activities with trace level Fe-doping in Ni and Co-layered double hydroxides for overall water splitting (<https://doi.org/10.1021/acsmami.8b16425>).
- [140] Z. Wu, Z. Zou, J. Huang, F. Gao, NiFe₂O₄ Nanoparticles/NiFe Layered Double-Hydroxide Nanosheet Heterostructure Array for Efficient Overall Water Splitting at Large Current Densities (<https://doi.org/10.1021/acsmami.8b07835>).
- [141] W. Mai, Q. Cui, Z. Zhang, K. Zhang, G. Li, L. Tian, W. Hu, CoMoP/NiFe-Layered Double-Hydroxide Hierarchical Nanosheet Arrays Standing on Ni Foam for Efficient Overall Water Splitting, *ACS Appl. Energy Mater.* 3 (2020) 8075–8085, <https://doi.org/10.1021/acsaem.0c01538>.
- [142] P. Wang, J. Qi, X. Chen, C. Li, W. Li, T. Wang, C. Liang, Three-Dimensional Heterostructured NiCoP@NiMn-Layered Double Hydroxide Arrays Supported on Ni Foam as a Bifunctional Electrocatalyst for Overall Water Splitting, *ACS Appl. Mater. Interfaces* 12 (2020) 4385–4395, <https://doi.org/10.1021/acsmami.9b15208>.
- [143] R.B. Mammar, L. Hamadou, Highly broadband plasmonic Pt nanoparticles modified α -Fe₂O₃/TiO₂ nanotubes for efficient photoelectrochemical water splitting, *Opt. Mater.* 143 (2023) 114191, <https://doi.org/10.1016/j.optmat.2023.114191>.
- [144] M.M. Abouelela, G. Kawamura, A. Matsuda, Metal chalcogenide-based photoelectrodes for photoelectrochemical water splitting, *J. Energy Chem.* 73 (2022) 89–213, <https://doi.org/10.1016/j.jechem.2022.05.022>.
- [145] Q.L. Mo, S. Hou, Z.Q. Wei, X.Y. Fu, G. Xiao, F.X. Xiao, Fine tuning of charge motion over homogeneous transient metal chalcogenides heterostructured photoanodes for photoelectrochemical water splitting, *J. Chem. Eng.* 433 (2022) 133641, <https://doi.org/10.1016/j.cej.2021.133641>.
- [146] S.N.F. Moridon, K. Arifin, R.M. Yunus, L.J. Minggu, M.B. Kassim, Photocatalytic water splitting performance of TiO₂ sensitized by metal chalcogenides: A review, *Ceram. Int.* 48 (2022) 5892–5907, <https://doi.org/10.1016/j.ceramint.2021.11.199>.
- [147] H.K. Zafar, M. Sohail, A. Nafady, K.K. Ostrikov, G. Will, M.A. Wahab, A. P. O'Mullane, S-doped copper selenide thin films synthesized by chemical bath deposition for photoelectrochemical water splitting, *Appl. Surf. Sci.* 641 (2023) 641,158505, <https://doi.org/10.1016/j.apsusc.2023.158505>.
- [148] T.H. Wang, T.K.A. Nguyen, R.A. Doong, Phosphorene nanosheet decorated graphitic carbon nitride nanofiber for photoelectrochemically enhanced hydrogen evolution from water splitting, *J. Taiwan Inst. Chem. Eng.* 141 (2022) 104577, <https://doi.org/10.1016/j.jtice.2022.104577>.
- [149] Q. Liu, T. Sun, L. Di, B. Xue, Amorphous molybdenum sulfide/polymeric carbon nitride composite with multiple interfaces for boosting photoelectrochemical water splitting performance, *Appl. Surf. Sci.* 640 (2023) 158404, <https://doi.org/10.1016/j.apsusc.2023.158404>.
- [150] X. Chia, A. Adriano, P. Lazar, Z. Sofer, J. Luxa, M. Pumera, Layered platinum dichalcogenides (PtS₂, PtSe₂, and PtTe₂) electrocatalysis: monotonic dependence on the chalcogen size, *Adv. Funct. Mater.* 26 (26) (2016) 4306–4318, <https://doi.org/10.1002/adfm.201505402>.
- [151] A. Singh, J. Rohilla, M.S. Hassan, C.T. Devaiah, P.P. Ingole, P.K. Santra, D. Ghosh, S. Sapra, MoSe₂/SnS Nanoheterostructures for Water Splitting, *ACS Appl. Nano Mater.* 5 (3) (2022) 4293–4304, <https://doi.org/10.1021/acsm.2c00233>.
- [152] R.B. Wei, P.Y. Kuang, H. Cheng, Y.B. Chen, J.Y. Long, M.Y. Zhang, Z.Q. Liu, Plasmon-Enhanced Photoelectrochemical Water Splitting on Gold Nanoparticle Decorated ZnO/CdS Nanotube Arrays, *ACS Sustain. Chem. Eng.* 5 (2017) 42494257, <https://doi.org/10.1021/acssuschemeng.7b00242>.
- [153] I.H. Kwak, H.S. Im, M.J. Jang, Y.W. Kim, K. Park, Y.R. Lim, E.H. Cha, J. Park, CoSe₂ and NiSe₂ Nanocrystals as Superior Bifunctional Catalysts for Electrochemical and Photoelectrochemical Water Splitting, *J. ACS Appl. Mater. Interfaces* 8 (8) (2016) 5327–5334, <https://doi.org/10.1021/acsm.5b12093>.